

THE SIMULATION OF
HYDROFOIL PERFORMANCE

DEC 74

Jitt Na Nagara

DUDLEY KNOX LIBRARY
NAVAL POSTGRADUATE SCHOOL
MONTEREY, CALIF. 94034

NAVAL POSTGRADUATE SCHOOL

Monterey, California



THESIS

THE SIMULATION OF
HYDROFOIL PERFORMANCE

by

Jitt Na Nagara

December 1974

Thesis Advisor:

George J. Thaler

Approved for public release; distribution unlimited.

T165264

REPORT DOCUMENTATION PAGE		READ INSTRUCTIONS BEFORE COMPLETING FORM
1. REPORT NUMBER	2. GOVT ACCESSION NO.	3. RECIPIENT'S CATALOG NUMBER
4. TITLE (and Subtitle) THE SIMULATION OF HYDROFOIL PERFORMANCE		5. TYPE OF REPORT & PERIOD COVERED Master's Thesis; December 1974
		6. PERFORMING ORG. REPORT NUMBER
7. AUTHOR(s) Jitt Na Nagara		8. CONTRACT OR GRANT NUMBER(s)
9. PERFORMING ORGANIZATION NAME AND ADDRESS Naval Postgraduate School Monterey, California 93940		10. PROGRAM ELEMENT, PROJECT, TASK AREA & WORK UNIT NUMBERS
11. CONTROLLING OFFICE NAME AND ADDRESS Naval Postgraduate School Monterey, California 93940		12. REPORT DATE December 1974
		13. NUMBER OF PAGES 103
14. MONITORING AGENCY NAME & ADDRESS (if different from Controlling Office) Naval Postgraduate School Monterey, California 93940		15. SECURITY CLASS. (of this report) Unclassified
		15a. DECLASSIFICATION/DOWNGRADING SCHEDULE
16. DISTRIBUTION STATEMENT (of this Report) Approved for public release; distribution unlimited.		
17. DISTRIBUTION STATEMENT (of the abstract entered in Block 20, if different from Report)		
18. SUPPLEMENTARY NOTES		
19. KEY WORDS (Continue on reverse side if necessary and identify by block number) Hydrofoil Simulation		
20. ABSTRACT (Continue on reverse side if necessary and identify by block number) The behavior of a fully-submerged hydrofoil has been studied by using Root Locus technique. A multivariable concept was used in designing the compensators of the system. A digital computer simulation program using Digital Simulation Language or DSL is produced to study the performance on the digital computer IBM system 360/67. The Highpoint PC(H)-1 is used as the model of this simulation.		

DD Form 1473 (BACK)
1 Jan 73
S/N 0102-014-6601

The Simulation of
Hydrofoil Performance

by

Jitt Na Nagara
Lieutenant, Royal Thai Navy
B.Sc., Royal Thai Naval Academy, 1964

Submitted in partial fulfillment of the
requirements for the degree of

MASTER OF SCIENCE IN ELECTRICAL ENGINEERING

from the

NAVAL POSTGRADUATE SCHOOL
December 1974

Thesis
N 3

ABSTRACT

The behavior of a fully-submerged hydrofoil has been studied by using Root Locus technique. A multivariable concept was used in designing the compensators of the system. A digital computer simulation program using Digital Simulation Language or DSL is produced to study the performance on the digital computer IBM system 360/67. The Highpoint PC(H)-1 is used as the model of this simulation.

TABLE OF CONTENTS

I.	INTRODUCTION -----	14
	A. FOIL TYPES -----	14
	B. FOIL ARRANGEMENT -----	16
II.	HYDROFOIL EQUATIONS STUDY -----	21
	A. COORDINATE SYSTEMS -----	21
	B. EQUATION OF MOTION -----	23
	C. CALCULATION OF VELOCITY COMPONENTS -----	27
	D. ANGLE OF ATTACK AND ANGLE OF SIDE SLIP -----	30
	E. EXPANSION OF FORCE AND MOMENT TERMS -----	32
	F. SPECIFICATION OF UNITS -----	34
III.	HYDROFOIL SIMULATION -----	35
	A. SIMULATION OBJECTIVE -----	35
	B. COMPUTER SIMULATION -----	36
	C. AUTOMATIC CONTROL -----	38
	1. Vertical Gyros -----	38
	2. Rate Gyros -----	39
	3. Accelerometer -----	39
	4. Height Sensor -----	40
IV.	TRANSFER FUNCTION AND ROOT LOCUS DESIGN -----	41
	A. PITCH-HEAVE MOTION TRANSFER FUNCTION -----	41
	B. ROOT LOCUS DESIGN OF FORWARD FOIL AUTOMATIC CONTROL -----	49
	C. ROOT LOCUS DESIGN OF AFT FOIL AUTOMATIC CONTROL -----	54

V.	MULTIVARIABLE SYSTEM -----	60
A.	BASIC CONCEPT -----	60
1.	The Characteristic Equation -----	61
2.	Connection Between Single-Loop and Multivariable -----	62
B.	ROOT LOCUS DESIGN FOR PITCH-HEAVE MODE -----	63
C.	ROOT LOCUS DESIGN FOR ROLL MODE -----	76
VI.	CONCLUSIONS AND RECOMMENDATIONS FOR FURTHER STUDY-	82
APPENDIX A	SUMMARY OF COMPLETE EQUATIONS -----	84
APPENDIX B	PLOTS OF HYDRODYNAMIC COEFFICIENTS -----	89
COMPUTER PROGRAMS	-----	93
LIST OF REFERENCES	-----	101
INITIAL DISTRIBUTION LIST	-----	102

LIST OF DRAWINGS

1	TYPE OF HYDROFOIL CRAFT -----	14
2	FOILS CONFIGURATION -----	17
3-A	FOIL IN CANARD ARRANGEMENT -----	18
3-B	FOIL IN AIRPLANE ARRANGEMENT -----	18
4-A	DRAWING OF FOIL AND STRUT CONFIGURATION -----	19
4-B	DRAWING OF FOIL AND FLAP CONFIGURATION -----	20
5	ORIENTATION OF THE BODY AXES WITH RESPECT TO THE CRAFT AND DIRECTIONS OF POSITIVE VELOCITIES -----	21
6	DEFINITION OF POSITIVE DIRECTIONS OF EULER ANGLE --	26
7	DEFINITION OF SYMBOLOGY -----	28
8-A	ANGLE OF ATTACK -----	31
8-B	ANGLE OF SIDESLIP -----	31
9	BLOCK DIAGRAM OF EQUATION RELATIONSHIPS -----	37
10	ROOT LOCUS PLOT OF $G_{p_{11}}$ -----	50
11	ROOT LOCUS PLOT OF $G_{p_{21}}$ -----	51
12	ROOT LOCUS PLOT OF $G_{p_{12}}$ -----	52
13	ROOT LOCUS PLOT OF $G_{p_{22}}$ -----	53
14	BLOCK DIAGRAM SHOWING FORWARD FOIL AUTOMATIC CONTROL -----	54
15	STEP RESPONSE OF THE CRAFT (FORWARD FOIL ONLY) ----	55
16	BLOCK DIAGRAM SHOWING AFT. FOIL AUTOMATIC CONTROL -	56
17	STEP RESPONSE OF THE CRAFT (AFT FOIL ONLY, INPUT = 2.0) -----	57
18	STEP RESPONSE OF THE CRAFT (AFT FOIL ONLY, INPUT = 0.5) -----	59

19	BLOCK DIAGRAM SHOWING A MULTIVARIABLE SYSTEM WITH DIAGONAL MATRIX CASCADE COMPENSATOR -----	61
20	ROOT LOCUS PLOT OF $1+G_{p_{11}} \cdot G_{c_{11}}$ -----	65
21	ROOT LOCUS PLOT OF $1+(\det \cdot G_p / G_{p_{22}}) \cdot G_{c_{11}}$ -----	66
22	ROOT LOCUS PLOT OF $1+G_{eq} \cdot G_{c_{22}}$ -----	70
23	BLOCK DIAGRAM SHOWING THE COMPENSATED SYSTEM -----	71
24	STEP RESPONSE OF HEIGHT (2 FT. UP) -----	72
25	STEP RESPONSE OF HEIGHT (2 FT. DOWN) -----	73
26	STEP RESPONSE OF PITCH ANGLE (BOW UP) -----	74
27	STEP RESPONSE OF PITCH ANGLE (STERN UP) -----	75
28	ROOT LOCUS PLOT OF ROLLING TRANSFER FUNCTION -----	78
29	STEP RESPONSE OF ROLL ANGLE (PORT UP) -----	79
30	STEP RESPONSE OF ROLL ANGLE (STARBOARD UP) -----	80
31	BLOCK DIAGRAM OF CONTROL SYSTEM -----	81

TABLE OF SYMBOLS

A_F	FEET ²	Area of foil
A_S	FEET ²	Area of strut
CG	- -	Center of gravity
C_{DF}	Dimensionless	Drag coefficient of a foil
C_{DS}	Dimensionless	Drag coefficient of a strut
C_L	Dimensionless	Lift coefficient
C_S	Dimensionless	Side force coefficient
F_{DiF}	Pounds	Drag force on a foil (water axes)
F_{DiS}	Pounds	Drag force on a strut (water axes)
F_{LiF}	Pounds	Lift force on foil (water axes)
F_{SiS}	Pounds	Side force on a strut (water axes)
F_X	Pounds	Force in direction of body X-axis
F_{XiF}	Pounds	Force on a foil in body X-axis
F_Y	Pounds	Force in body Y-axis
F_{YiF}	Pounds	Force on a foil in body Y-axis
F_{YiS}	Pounds	Force on a strut in body Y-axis
F_Z	Pounds	Force in direction of body Z-axis
F_{ZiF}	Pounds	Force on a foil in body Z-direction
F_{ZiS}	Pounds	Force on a strut in body Z-direction
g_X	Feet/Second ²	Component of gravity in body X-direction
g_Y	Feet/Second ²	Component of gravity in body Y-direction
g_Z	Feet/Second ²	Component of gravity in body Z-direction

h_S	Feet	Height of Height Sensor above instantaneous water surface
I_{XX}	Slug-Foot ²	Moment of inertia about body X-axis
I_{YY}	Slug-Foot ²	Moment of inertia about body Y-axis
I_{ZZ}	Slug-Foot ²	Moment of inertia about body Z-axis
L	Foot-Pound	Moment acting to produce roll about body X-axis
L_{XHS}	Feet	Distance from CG. along X-axis to a point of application of foil force
L_{XiF}	Feet	Distance from CG. along X-axis to a point of foil force
L_{YiF}	Feet	Distance from CG. along body Y-axis to a point of application of foil force
L_{ZiF}	Feet	Distance from CG. along body Z-axis to a point of application of foil force
L_{ZiS}	Feet	Distance from CG. along body Z-axis to a point of application of strut force
M	Foot-Pounds	Moment acting to provide pitch about body X-axis

m	Slugs	Mass of the craft
N	Foot-Pounds	Moment acting to produce yaw about body Z-axis
P	Radians/Second	Roll rate about body X-axis
Q	Radians/Second	Pitch rate about body Y-axis
R	Radians/Second	Yaw rate about body Z-axis
S_{EiF}	Feet	Submergence of a foil in earth axes
S_{EiS}	Feet	Submergence in earth axes of the assumed point of application of strut force
SHP	Horsepower	Shaft horsepower
T_X	Pounds	Magnitude of thrust in direction of body X-axis
U	Feet/Second	Velocity in direction of body X-axis
U_E	Feet/Second	Velocity along earth X-axis
U_i	Feet/Second	Foil velocity in direction of body X-axis
V	Feet/Second	Velocity in direction of body Y-axis
V_E	Feet/Second	Velocity along earth Y-axis
V_i	Feet/Second	Foil velocity in direction of body Y-axis
W	Feet/Second	Velocity in direction of body Z-axis
W_E	Feet/Second	Velocity along earth Z-axis
W_i	Feet/Second	Foil velocity in direction of body Z-axis

X_E	Feet	Distance along earth X-axis from reference origin
Y_E	Feet	Distance along earth Y-axis from reference origin
α_i	Radians	Angle of attack of a particular foil, designated by subscript
β_i	Radians	Angle of side slip of particular strut, designated by subscript
η	Dimensionless	Propulsion efficiency
ρ	Slugs/Foot ³	Water density
ϕ	Radians	Roll angle
ψ	Radians	Yaw angle
θ	Radians	Pitch angle

Subscripts

C	Refers to Center foil or strut
P	Refers to Port foil or strut
S	Refers to Starboard foil or strut
M	Refers to Mid foil section
F	Refers to foil
S	Refers to strut
i	When "i" appears in the subscript to a symbol, it indicates that the symbol is to be repeated with i successfully replaced by C, P, S, and M, as indicated.

ACKNOWLEDGEMENT

I would like to express my deepest appreciation for Dr. George J. Thaler's considered advice and help. For without them, this research paper would not have been possible.

I. INTRODUCTION

A. FOIL TYPES

The main idea of the hydrofoil craft is to reduce the resistance of the craft by reducing the area in contact with the water and thus increase the speed for the same power. One way to accomplish this is fitting foils below the hull of a craft, so that the craft is lifted clear of the water at high speed. There are two principal foil arrangements in use today, classed as surface piercing foil and fully-submerged foil, as shown in Figure 1.

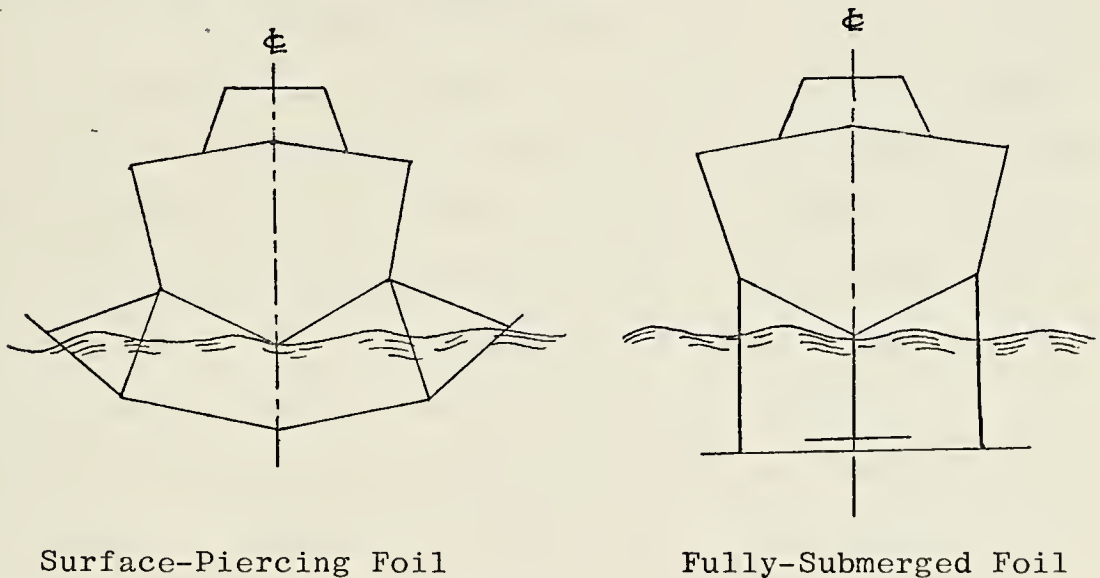


FIGURE 1

TYPE OF HYDROFOIL CRAFT

The surface-piercing foil is supported by vertical struts and the lifting surface extends in a V-shape from the water surface down through the water to the point of convergence of the V. The surface-piercing foil provides a

self-stabilization for the craft in pitch, height and roll. The self-stabilizing aspect of the surface piercing foil is easy to see. Suppose the craft pitches up slightly, then less area of the forward foil and more area of the after foil is submerged. This results in less lift from the forward foil and more lift from the after foil so the craft will settle back again, the same stabilization occurs in roll. For the height as the craft speed increases the whole craft rises up until the amount of wetted surface of the foils is just sufficient to create a lift equal to the weight of the craft.

The fully-submerged foil cannot adjust itself to changing lift demands by a change in area, but only by a change in incidence, either of the whole foil or of attached flaps. This involves the use of some sensing arrangement to control the incidence by monitoring the height of the craft above water surface. The fully-submerged foil is a more sophisticated design, and the control mechanism is likely to be complicated. But the fully-submerged foil has a very distinct advantage when operating in heavy seas. The surface-piercing foil will respond to even relatively small changes in the surface of the sea and give a very rough ride. The fully-submerged foil, on the other hand, is much less affected by the change in the surface of the sea. This paper will deal only with the fully-submerged foil craft.

B. FOIL ARRANGEMENT

Most of the fully-submerged foil craft have two foils, one at the forward and the other at the aft. Both foils are supported by the vertical struts. Figure 2 shows the configuration of main foil and secondary foil; Figures 3A and 3B show foils in canard arrangement and in airplane arrangement respectively.

The simulation in this paper is based on the canard arrangement, which has a secondary foil as a forward foil and a main foil as the aft foil. The HIGH POINT PC(H)-1 was the model for this simulation. Drawing of the craft and the foils are shown in Figures 4A and 4B.

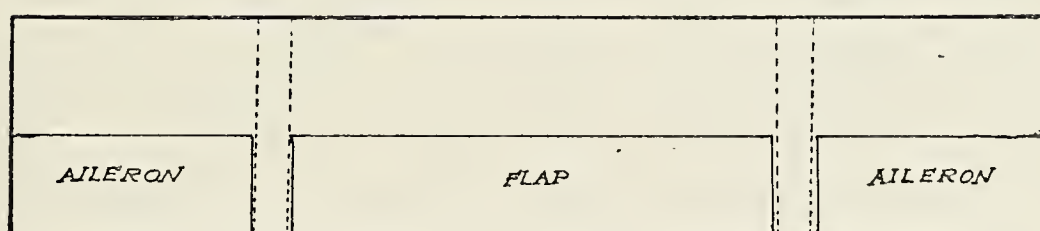
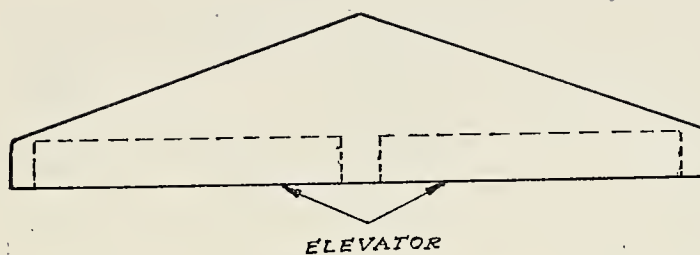


FIGURE 2
FOILS CONFIGURATION

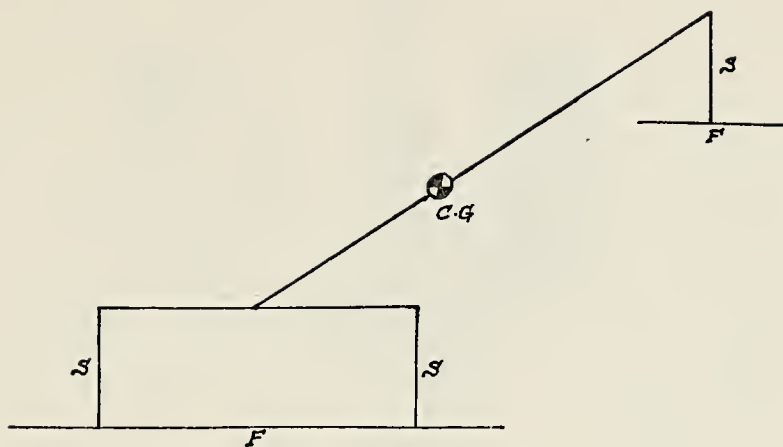


FIGURE 3A
FOIL IN CANARD ARRANGEMENT

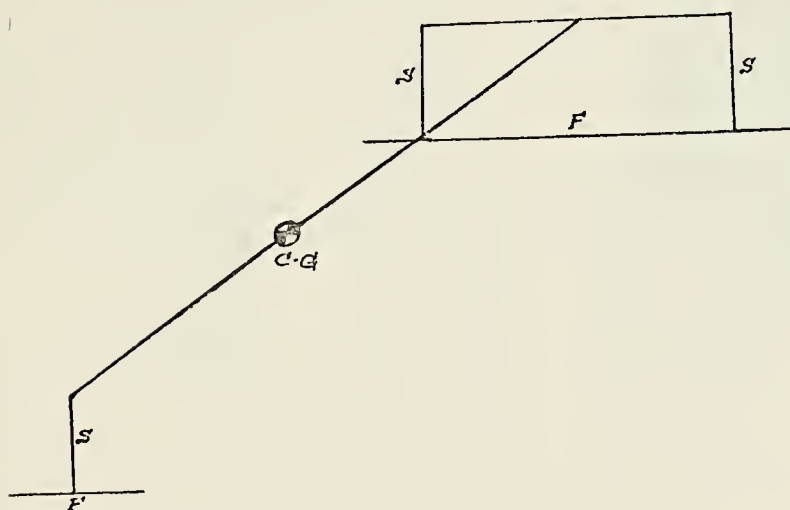
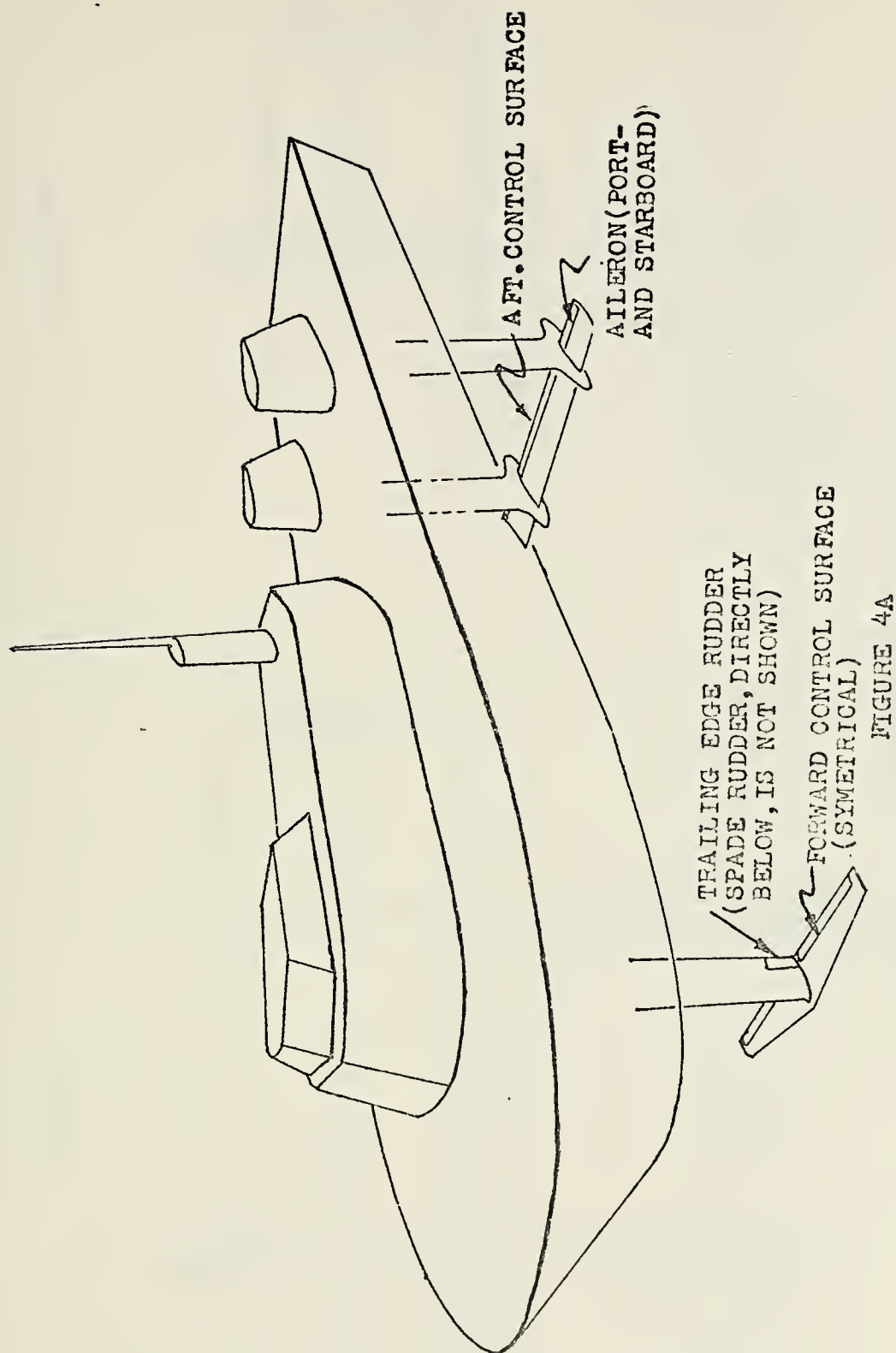
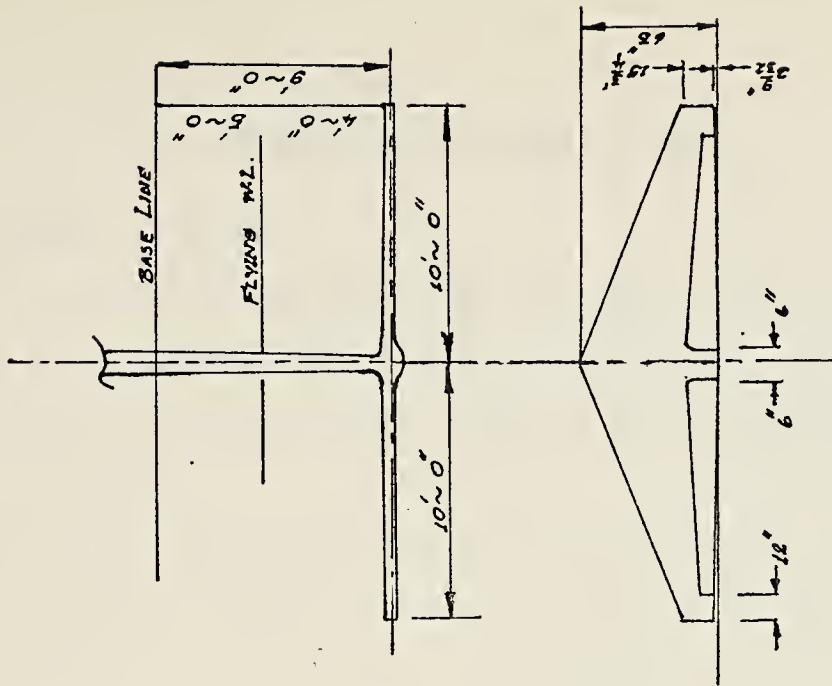


FIGURE 3B
FOIL IN AIRPLANE ARRANGEMENT



DRAWING OF FOIL AND STRUT CONFIGURATION

FORWARD FOIL



AFT FOIL

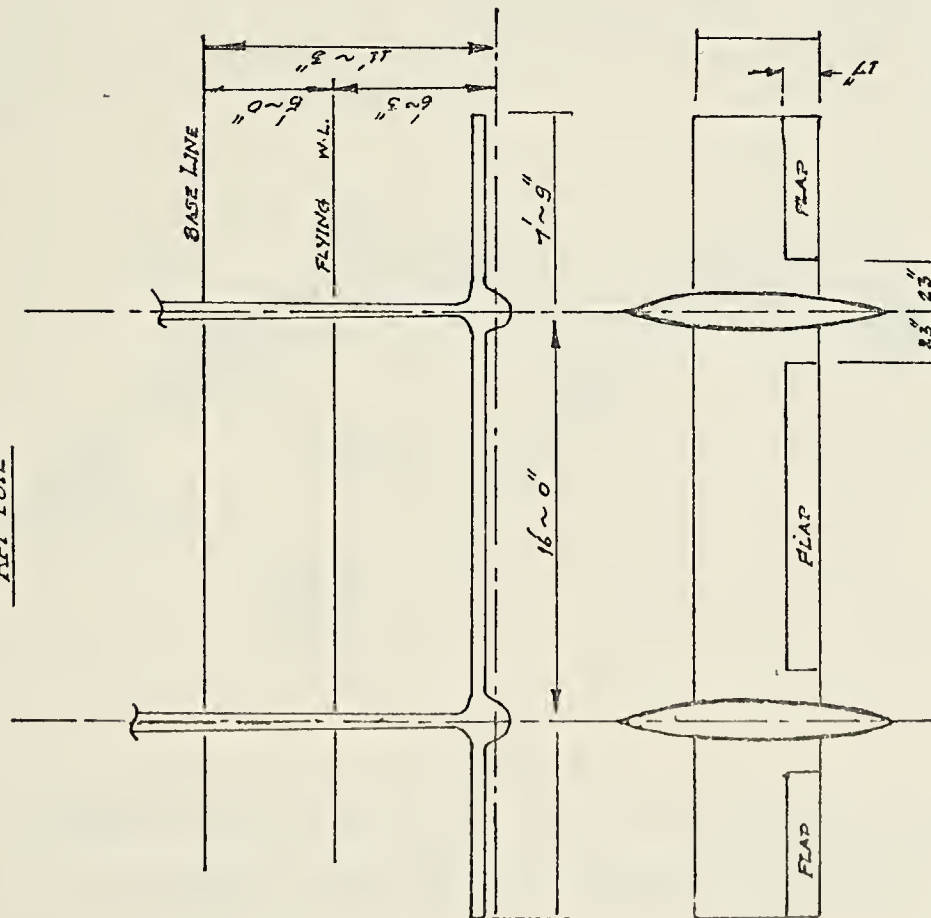


FIGURE 4B
DRAWING OF FOIL AND FLAP CONFIGURATION

II. HYDROFOIL EQUATIONS STUDY

A. COORDINATE SYSTEMS

Three coordinate systems will be used in this study of hydrofoil craft dynamics. They are: the Body Axes, the Water Axes and the Earth Axes. Each is in a right hand orthogonal system.

The body axes coordinate system (x, y, z) shown in Figure 5 has its origin at the center of gravity of the craft and is fixed relative to the craft. This system is initially coincident with the origin of the earth axes system, however, it moves with the craft as time progresses. X is positive forward, Y is positive to starboard and Z is positive downward.

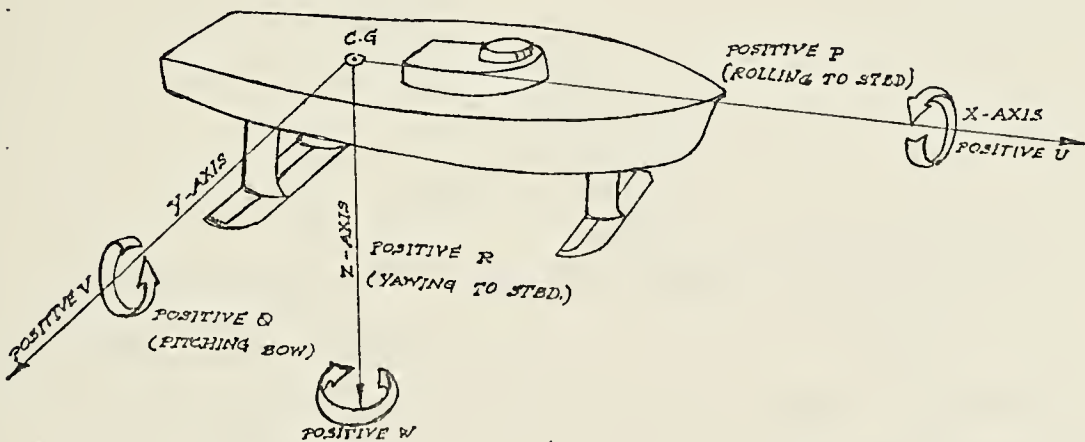
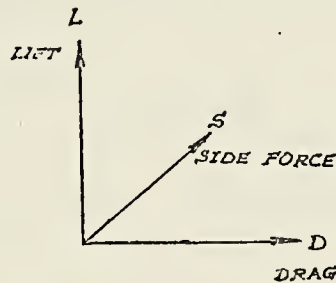


FIGURE 5

ORIENTATION OF THE BODY AXES WITH RESPECT TO THE
CRAFT AND DIRECTIONS OF POSITIVE VELOCITIES

The earth axes coordinate system (X_E, Y_E, Z_E) is fixed relative to the earth surface. The origin may be chosen at any convenient location, provided the body system origin is initially at the same point. The X_E axis lies in the horizontal plane; it is initially coincident with, and positive in the same direction as the body X axis. The Y_E axis lies in the horizontal plane and is positive to starboard when the observer is facing the positive X_E direction. The Z_E axis is normal to the horizontal and is positive downward. Water surface motion and craft motion relative to calm water are described in this coordinate system.

The water axes coordinate system is aligned with the relative velocity vector and resolves into "Lift," "Drag," and Side-Force" direction.



It will be specified that the order of rotation from water axes to body axes is:

- 1) The (D,S) axes rotate about the L-axis through the angle β to the position (D_1, S_1) where S_1 is coincident with the body Y-axis.
- 2) The (D_1, L) axes rotate about the S_1 -axis, or more pertinently about the Y-axis, through the angle α to the position (D_2, L_1) which corresponds to the ($-X, -Z$) axes.

B. EQUATION OF MOTION

The development of the six equations of motion for a hydrofoil follows the same procedure as those for a displacement type hull. This development is clearly outlined in Ref. 2 and 8 and therefore will not be done here.

The equations of motion are:

Translation

$$\dot{u} = \frac{1}{m}F_X - QW + RV \quad (2-1)$$

$$\dot{v} = \frac{1}{m}F_Y + PW - RU \quad (2-2)$$

$$\dot{w} = \frac{1}{m}F_Z + QU - PV \quad (2-3)$$

Rotation

$$\dot{P} = \frac{1}{I_{XX}}[L - QR(I_{ZZ} - I_{YY}) + (\dot{R} + QP)I_{XZ}] \quad (2-4)$$

$$\dot{Q} = \frac{1}{I_{YY}}[M - RP(I_{XX} - I_{ZZ}) - (P^2 - R^2)I_{XZ}] \quad (2-5)$$

$$\dot{R} = \frac{1}{I_{ZZ}}[N - PQ(I_{YY} - I_{XX}) - (QR - \dot{P})I_{XZ}] \quad (2-6)$$

The terms RV, PV, and PW are very small and may be neglected. Similarly, the product of inertia quantity, I_{XZ} , is less than 10% of I_{XX} and less than 4% of I_{ZZ} . Consequently, when considered in conjunction with the magnitudes of $(\dot{R} + PQ)$, $(P^2 - R^2)$ and $(QR - \dot{P})$, the terms containing I_{XZ} may be neglected for this craft.

Equations (2-1) through (2-6) are linear and rotational accelerations in body axes. The velocity terms in body axes

can be obtained directly by integrating each equation one time.

$$U = \int \dot{U} dt \quad (2-7)$$

$$V = \int \dot{V} dt \quad (2-8)$$

$$W = \int \dot{W} dt \quad (2-9)$$

$$P = \int \dot{P} dt \quad (2-10)$$

$$Q = \int \dot{Q} dt \quad (2-11)$$

$$R = \int \dot{R} dt \quad (2-12)$$

Linear displacements and angular positions with respect to body axes could be obtained by an additional integration, but such quantities are of limited usefulness. The displacements and angle usually of interest are those with respect to earth axes. In order to calculate the craft's position in earth axes coordinates, the craft velocity vector must be transformed from body axes coordinates into earth axes coordinates as follow:

$$\begin{aligned} U_E = & U \cos \theta \cos \psi + V [\cos \psi \sin \theta \sin \phi - \sin \psi \cos \phi] \\ & + W [\cos \psi \sin \theta \cos \phi + \sin \psi \sin \phi] \end{aligned} \quad (2-13)$$

$$\begin{aligned} V_E = & U \cos \theta \sin \psi + V [\cos \psi \cos \phi + \sin \psi \sin \theta \sin \phi] \\ & + W [\sin \psi \sin \theta \cos \phi - \cos \psi \sin \phi] \end{aligned} \quad (2-14)$$

$$W_E = -U \sin \theta + V \cos \theta \sin \phi + W \cos \theta \cos \phi \quad (2-15)$$

Only the craft's velocity in the downward, Z_E , direction is required to calculate its height above the water surface. That is, the vertical position in earth axes follows from

$$Z_E = \int W_E dt \quad (2-16)$$

The craft's position coordinates are obtained from

$$X_E = \int U_E dt \quad (2-17)$$

$$Y_E = \int V_E dt \quad (2-18)$$

The Euler angles, ϕ , θ , and ψ are also of interest and can be found by integration of Euler rates $\dot{\phi}$, $\dot{\theta}$, and $\dot{\psi}$. The rates in turn must be derived from the body angular rates. The Euler rates are not easily obtained because they occur about axes which are not orthogonal. This fact can be appreciated by referring to Figure 6 and recalling how the angles were defined. ψ is a rotation about the Z_0 axis, θ is a rotation about the Y_1 axis, and ϕ is a rotation about the X axis. They result in the following set of equations:

$$\dot{\phi} = P + \dot{\psi} \sin \theta \quad (2-19)$$

$$\dot{\theta} = Q \cos \phi - R \sin \phi \quad (2-10)$$

$$\dot{\psi} = (Q \sin \phi + R \cos \phi) \cos \theta + (\dot{\phi} - P) \sin \theta \quad (2-21)$$

Studies of this craft show that even under the most drastic abnormal situations, pitch angles are not expected to reach 10° and under normal operating conditions, roll angles will not exceed 3° . Therefore, the following assumptions are justified;

$$\begin{aligned} \sin \theta &= 0 \\ \cos \theta &= 1 \end{aligned} \quad (2-22)$$

The Euler angles are obtained by integration of equations (2-19) through (2-21).

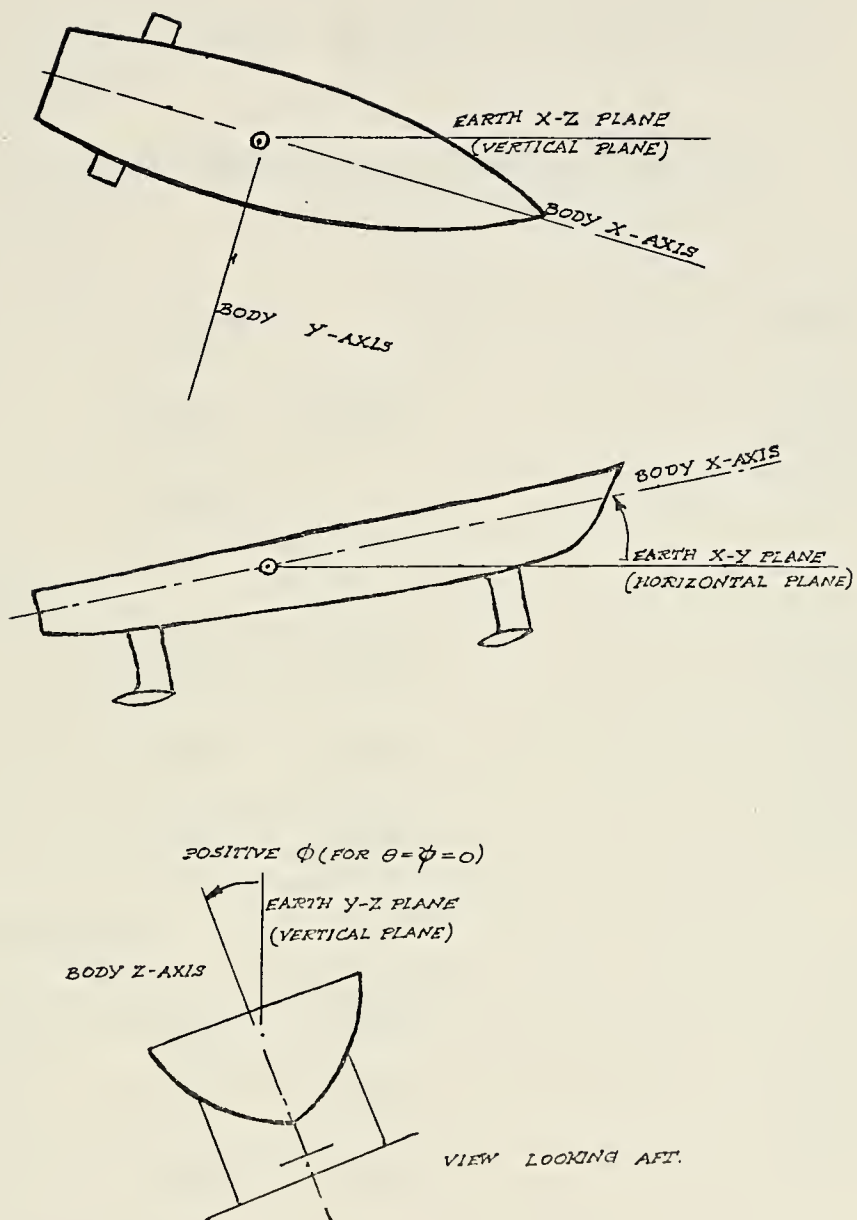


FIGURE 6

DEFINITION OF POSITIVE DIRECTIONS OF EULER ANGLE

C. CALCULATION OF VELOCITY COMPONENTS

The total velocity components of each foil in body axes can be expressed in terms of craft linear and angular velocities by considering the craft geometry as represented in Figure 7 and Table I.

The resultant equations for the example shown are:

Center Foil

$$U_C = U + L_{ZCF} \cdot Q \quad (2-23)$$

$$V_C = V - L_{ZCF} \cdot P + L_{XCF} \cdot R \quad (2-24)$$

$$W_C = W - L_{XCF} \cdot Q \quad (2-25)$$

Port Foil

$$U_P = U + L_{ZPF} \cdot Q - L_{YPF} \cdot R \quad (2-26)$$

$$V_P = V - L_{ZPF} \cdot P + L_{XPF} \cdot R \quad (2-27)$$

$$W_P = W + L_{YPF} \cdot P - L_{XPF} \cdot Q \quad (2-28)$$

Starboard Foil

$$U_S = U + L_{ZSF} \cdot Q - L_{YSF} \cdot R \quad (2-29)$$

$$V_S = V - L_{ZSF} \cdot P + L_{XSF} \cdot R \quad (2-30)$$

$$W_S = W + L_{YSF} \cdot P - L_{XSF} \cdot Q \quad (2-31)$$

Mid-Foil Segment

$$U_M = U + L_{ZMF} \cdot Q \quad (2-32)$$

$$V_M = V - L_{ZMF} \cdot P + L_{XMF} \cdot R \quad (2-33)$$

$$W_M = W - L_{XMF} \cdot Q \quad (2-34)$$

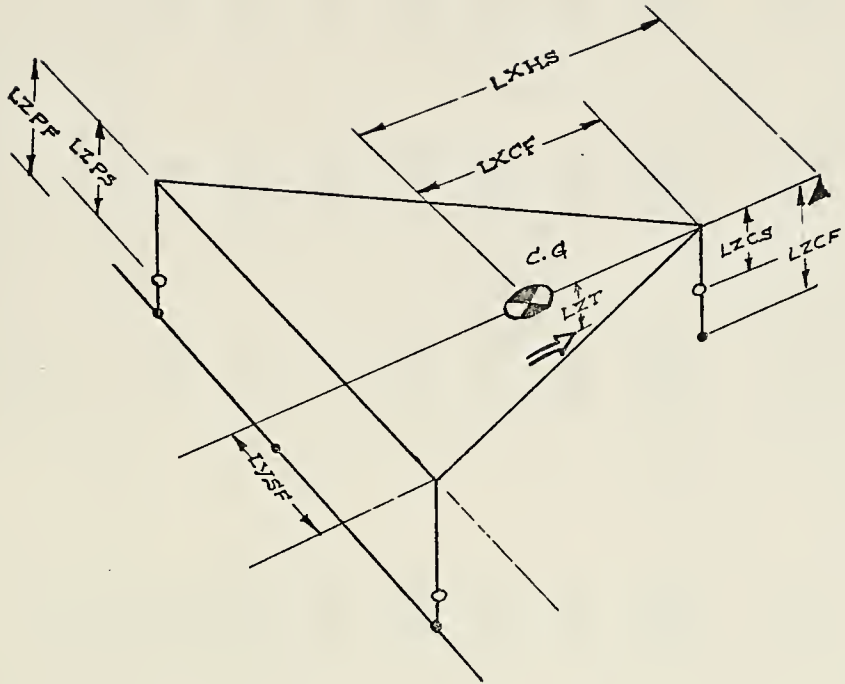


FIGURE 7

DEFINITION OF SYMBOLOGY

- = Point of application of foil forces
- = Point of application of strut forces

$$L_{XCF} = L_{XCS}$$

$$L_{XPF} = L_{XPS} = L_{XSF} = L_{XSS} = L_{XMF}$$

$$L_{YSF} = L_{YSS} = L_{YPF} = L_{YPS}$$

$$L_{ZPF} = L_{ZSF} = L_{ZMF}$$

L_{ZPS} and L_{ZSS} are variables and in general will not be equal.

TABLE I

Point of Application of Force	Symbol for Force Along or Parallel to			Coordinate From CG to Point of Application Relative to		
	X-Axis	Y-Axis	Z-Axis	X-Axis	Y-Axis	Z-Axis
Center Foil	F_{XCF}	F_{YCF}	F_{ZCF}	L_{XCF}	L_{YCF}	L_{ZCF}
Center Strut	F_{XCS}	F_{YCS}	F_{ZCS}	L_{XCS}	L_{YCS}	L_{ZCS}
Port Foil	F_{XPF}	F_{YPF}	F_{ZPF}	L_{XPF}	L_{YPF}	L_{ZPF}
Port Strut	F_{XPS}	F_{YPS}	F_{ZPS}	L_{XPS}	L_{YPS}	L_{ZPS}
Starboard Foil	F_{XSF}	F_{YSF}	F_{ZSF}	L_{XSF}	L_{YSF}	L_{ZSF}
Starboard Strut	F_{XSS}	F_{YSS}	F_{ZSS}	L_{XSS}	L_{YSS}	L_{ZSS}
Mid Foil Segment	F_{XMF}	F_{YMF}	F_{ZMF}	L_{XMF}	L_{YMF}	L_{ZMF}
Effective Point of Application of Prop. Thrust	T_X	0	T_Z	L_{XT}	0	L_{ZT}

These foil velocities are in body axis terms and can be used directly to calculate the angles of attack and angles of side slip.

D. ANGLE OF ATTACK AND ANGLE OF SIDE SLIP

The angle of attack of the foil is shown in Figure 8A and defined as the angle whose tangent is the total relative velocity between the water and the foil in the body Z direction, divided by the total relative velocity between the water and foil in the body X direction

$$\alpha = \text{arc tan } \frac{W_r}{U_r} \quad (2-35)$$

If the foil is not aligned with the body X-axis, then the foil has a fixed angle of attack and the total angle of attack becomes

$$\alpha_{\text{TOTAL}} = \alpha_{\text{FIXED}} + \alpha \quad (2-36)$$

The side slip angle is shown in Figure 8B and can be represented by

$$\beta_i = \text{arc tan } \frac{V_{ri}}{\sqrt{U_{ri}^2 + V_{ri}^2 + W_{ri}^2}} \quad (2-37)$$

During actual craft operations, the angles will be less than 10°, and will permit use of the small angle approximation. Also the V and W velocities can be considered very small in relation to the U velocity. Applying these simplifications, the equations for α and β become:

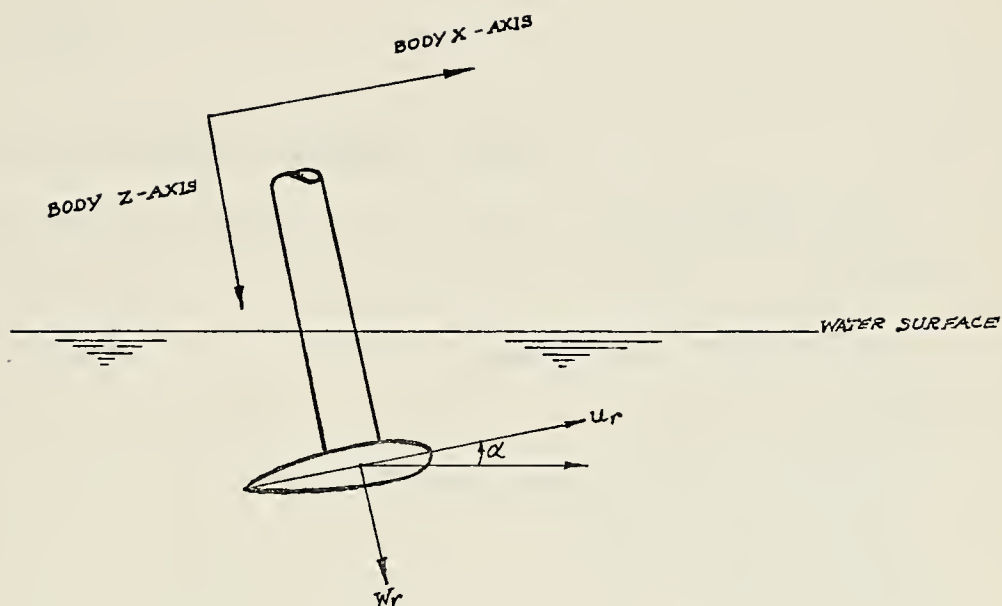


FIGURE 8A
ANGLE OF ATTACK

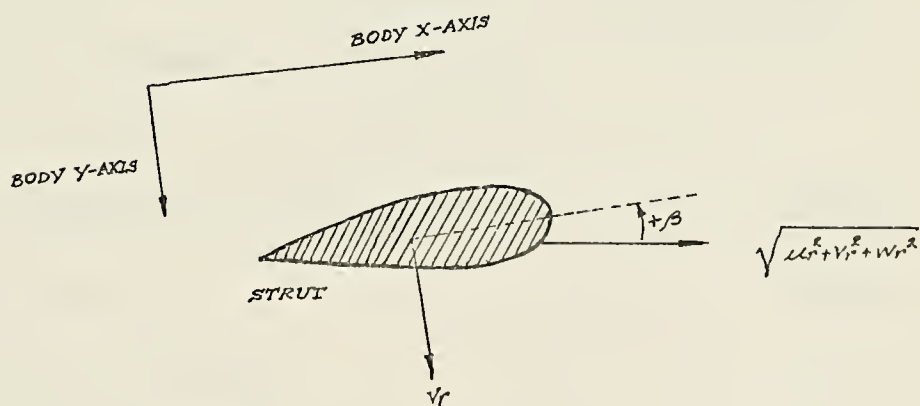


FIGURE 8B
ANGLE OF SIDE SLIP

$$\alpha_i = \frac{W_{ri}}{U} + \alpha_{i-FIXED}$$

$$\beta_i + \frac{V_{ri}}{U}$$

E. EXPANSION OF FORCE AND MOMENT TERMS

With the aid of Figure 7 and Table I, the forces and moments are set down. It is important that when a numerical value is inserted for one of the alphabetical dimensions, the sign of the value must be positive or negative according to positive and negative directions from the axis system origin at the C.G. Also note that horizontal foils make no contribution to the body Y force and vertical struts do not contribute to the body Z force. One of the assumptions made upon commencing simulation was that the struts contributed zero lift and that the foils contributed zero side force. Therefore, all body Y motion originates at the struts and all body Z motion originates at the foils.

The force and moment equations become:

$$F_X = F_{XCF} + F_{XPF} + F_{XSF} + F_{XCS} + F_{XSS} + m_{gx} + T_X \quad (2-38)$$

$$F_Y = F_{YCS} + F_{YPS} + F_{YSS} + m_{gy} \quad (2-39)$$

$$F_Z = F_{ZCF} + F_{ZPF} + F_{ZSF} + F_{ZMF} + m_{gz} \quad (2-40)$$

$$L = (F_{ZL_Y})_{PF} + (F_{ZL_Y})_{SF} - (F_{YL_Z})_{PS} - (F_{YL_Z})_{SS} - (F_{YL_Z})_{CS} \quad (2-41)$$

$$\begin{aligned} M = & -(F_{ZL_X})_{CF} - (F_{ZL_X})_{PF} - (F_{ZL_X})_{SF} - (F_{ZL_X})_{MF} + (F_{XL_Z})_{CF} \\ & + (F_{XL_Z})_{PF} + (F_{XL_Z})_{SF} + (F_{XL_Z})_{MF} + (F_{XL_Z})_{CS} + (F_{XL_Z})_{PS} \\ & + (F_{XL_Z})_{SS} + T_X L_{ZT} \end{aligned} \quad (2-42)$$

$$N = (F_{YL_X})_{CS} + (F_{YL_X})_{PS} + (F_{YL_X})_{SS} \quad (2-43)$$

All of these forces have a hydrodynamic origin except for the thrust and gravity terms. The thrust is always associated with the body axis and requires no further expansion. The gravity terms can be simplified using small angle approximation for the Euler angles (see equations A-31,32,33).

The general expression for hydrodynamic forces in water axes coordinates is

$$F_i = qAC_i \quad i = L,D,S \quad (2-44)$$

where L,D,S represent lift, drag and side force respectively. The lift, drag, and side force coefficients vary as functions of angle of attack, angle of side slip, submergence, velocity, flap elevator and rudder positions.

Ideally, mathematical expressions would have been developed to correctly depict the interrelation of all the variables which affect the force coefficients. However, hydrofoil technology has not advanced to a position which would yield such expressions. Some of the major problems encountered in deriving a mathematical expression are:

- 1) The occurrence of cavitation and ventilation which are completely unpredictable.
- 2) Even more unpredictable is the cessation of cavitation and ventilation.
- 3) The nonlinearity of the hydrodynamic coefficients.
- 4) Lack of sufficient test data to completely describe all of the above.

F. SPECIFICATION OF UNITS

Considerable confusion resulted from the interpretation of the various references concerning the units used in defining Euler angles and angular rotations. This problem has been alleviated here by the specific definitions in the Table of Symbols.

III. HYDROFOIL SIMULATION

A. SIMULATION OBJECTIVES

The object of the simulation was to commence the runs with the craft foilborne and in a steady state condition. Once this condition was achieved, the step response of the craft would be studied by applying step functions to excite motion along and about each body axis. That is, perturbations should be introduced to separately excite:

- 1) Motion along the X-axis
- 2) Motion about the X-axis
- 3) Motion along the Y-axis
- 4) Motion about the Y-axis
- 5) Motion along the Z-axis
- 6) Motion about the Z-axis

After the step response was obtained, a sinusoidal sea would be inserted to observe the craft's motion in a seaway. The following assumptions were made prior to beginning simulation:

- 1) Craft equations of motion are valid only for the foilborne mode.
- 2) Weight of the craft remains constant.
- 3) Hydrodynamic coefficients are based on fully wetted surfaces, i.e. no cavitation or ventilation.
- 4) No constraint was placed on craft's heading.

- 5) Foils are considered flat surfaces vice dihedral/
anhedral.
- 6) The craft may be operated in calm water or seaway.

B. COMPUTER SIMULATION

The computer language used in this simulation was Digital Simulation Language or DSL, and based on the computer program in Ref. 1.

Before the main program could be assembled, subroutines had to be written to find the hydrodynamic coefficients of foil lift and drag, and strut drag and side slip. Using the simulation curves in Ref. 3 as a guide, the curves were stored as data points in the setup routine. The subroutines "INTERP" and "INTERP1" are interpolation routines to obtain the proper coefficient from the curves. For INTERP, values of angle of attack and flap angle are used to enter the curves and obtain a value of foil drag. Angle of side slip and submergence are used to enter INTERP1 to obtain strut drag. The curve for the lift coefficient of a foil in the fully wetted region is straight line so this coefficient is found by merely solving the equation for the straight line. Curves plotted from the subroutines are shown in Appendix B. Listings of the subroutines are shown in the computer program section. The main program was then assembled using Figure 9 as a reference for data flow. One part before the end of the main program was opened for an automatic control block. A complete listing of the main program is shown in the computer program section.

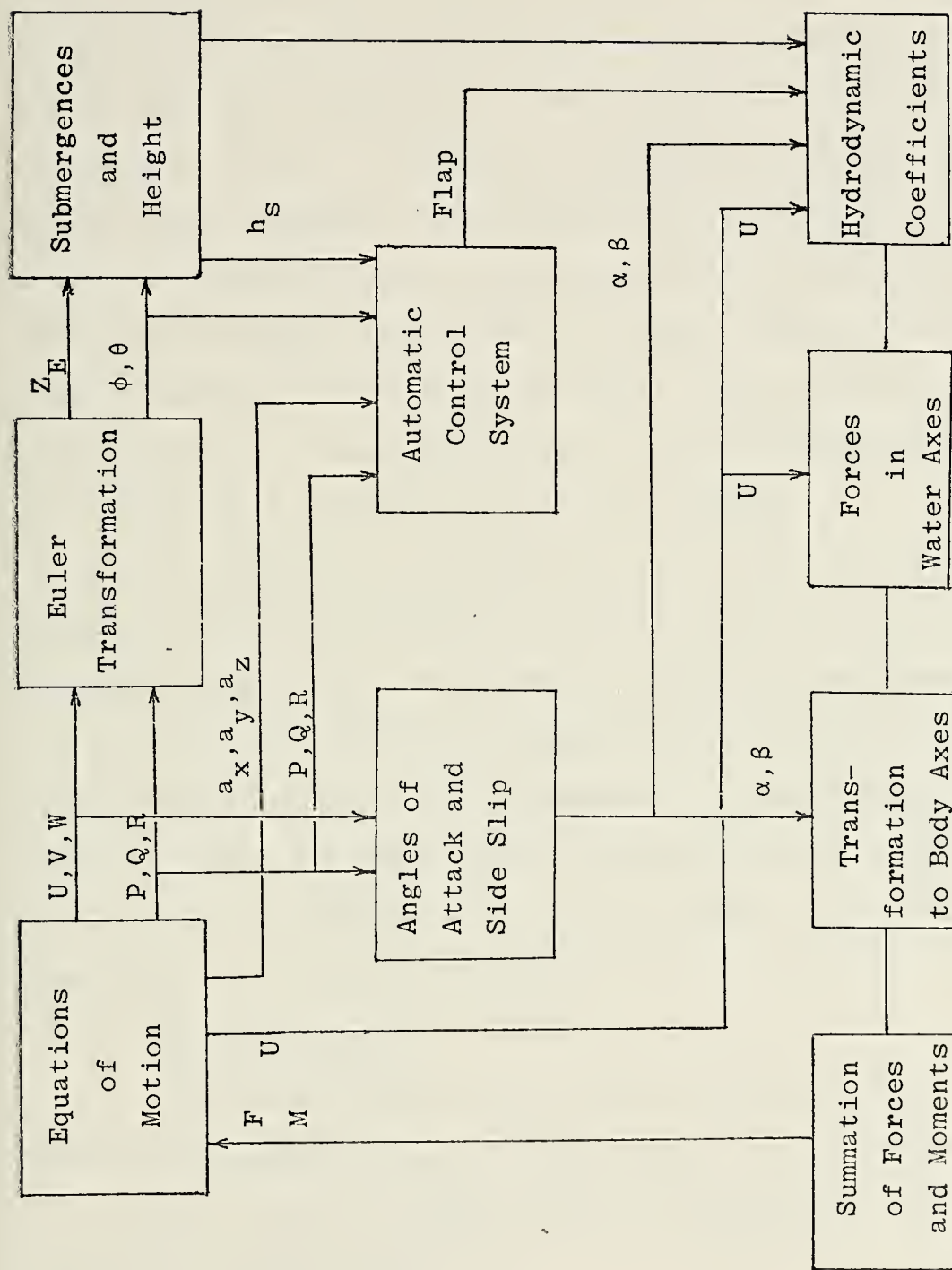


FIGURE 9

BLOCK DIAGRAM OF EQUATION RELATIONSHIPS

C. AUTOMATIC CONTROL

Control signals originate at the pilot's controls, at the motion sensors, and at the position transducer. These are combined and processed in the electronics to produce the signal for the servo-valve. The pilot will be able to move the helm, a lever, or a knob to introduce steering, altitude and attitude commands, the motion sensors sense errors between the commanded and actual craft motions and produce electrical signals proportional to these errors. The position transducer provides the feedback signal so that the control surface stops moving when it has reached the position corresponding to the processed error signals.

It is necessary to consider how the control system components affect the equations of motion through the control surface deflections. In general, a signal originating at the pilot or at the motion sensors will be modified by the individual dynamics of the components in the signal path before the control surface motion actually occurs. Motion sensors to be discussed are vertical gyros, rate gyros, accelerometers and height sensors.

1. Vertical Gyros

A vertical gyro of the type of interest here will produce one signal directly proportional to the pitch angle of the craft and one signal directly proportional to the roll angle of the craft.

2. Rate Gyros

A rate gyro will sense an angular rate about one of the three body axes. (Three-gyro "rate packages" are available if required for a particular application.) The dynamics of the gyro are such as to produce an output signal which is related to the actual angular rate by a second order differential equation. Using the roll rate P, as an example, the equation is

$$P = \frac{1}{\omega_n^2} \left(\frac{d^2 \tilde{P}}{dt^2} + 2\zeta \omega_n \frac{d\tilde{P}}{dt} + \omega_n^2 \tilde{P} \right) \quad (3-1)$$

or in transfer function form for all rotational rates:

$$\frac{\tilde{P}}{P} = \frac{\tilde{Q}}{Q} = \frac{\tilde{R}}{R} = \frac{\omega_n^2}{s^2 + 2\zeta \omega_n s + \omega_n^2} \quad (3-2)$$

where

$\tilde{P}, \tilde{Q}, \tilde{R}$ = Outputs of rate gyros (RAD/SEC)

P, Q, R = Craft rotational rates (RAD/SEC)

ω_n = Natural frequency of a particular gyro
(RAD/SEC)

ζ = Damping ratio of a particular gyro
(Dimensionless)

S = Laplace transform variable

3. Accelerometer

Outputs of accelerometers are also assumed to relate to the craft motions by second order differential equations. In general form, the equation is:

$$a_i = \frac{1}{\omega_n^2} \left(\frac{d^2 \tilde{a}_i}{dt^2} + 2\zeta \omega_n \frac{d\tilde{a}_i}{dt} + \omega_n^2 \tilde{a}_i \right) \quad (3-3)$$

or:

$$\frac{\tilde{a}_i}{a_i} = \frac{\omega_n^2}{S^2 + 2\zeta\omega_n S + \omega_n^2} \quad (3-4)$$

where i will become a symbol corresponding to the location of a particular accelerometer.

To identify the accelerations sensed by the instruments, it will be assumed that there is one accelerometer at the C.G. mounted such as to measure lateral acceleration, and one accelerometer above each foil mounted in the X-Y plane so as to measure accelerations parallel to the Z-axis.

The lateral acceleration at the C.G. is:

$$a_y = \frac{F_y}{m} \quad (3-5)$$

Taking angular acceleration into account, the accelerations in the Z-direction at points above a center, port, and starboard foil are:

$$A_{ZC} = \frac{F_Z}{m} - L_{XCF} \cdot \dot{Q} \quad (3-6)$$

$$A_{ZP} = \frac{F_Z}{m} + L_{XPF} \cdot \dot{Q} - L_{YPF} \cdot \dot{P} \quad (3-7)$$

$$A_{ZS} = \frac{F_Z}{m} + L_{XSF} \cdot \dot{Q} + L_{YSF} \cdot \dot{P} \quad (3-8)$$

4. Height Sensor

Ultrasonic and sonar types are either in use or expected to be used. For this study it will be assumed that the dynamic characteristics of the sensor, whatever the type, will be such as to give a direct indication of the instantaneous height of the sensor above the water.

IV. TRANSFER FUNCTION AND ROOT LOCUS DESIGN

A. PITCH-HEAVE MOTION TRANSFER FUNCTION

The best way to study the stability of the craft was to find the transfer functions of the craft and use either Root Locus plots or Bode plots to be an aid in a stability study and also in designing the compensators of the system.

The transfer functions of the craft can be derived directly from the equations of motion. In the pitch-heave mode, equations (2-3) and (2-5) were the equations that described the motion in the Z-axis and motion about the Y-axis. After neglecting the small terms, equations (2-3) and (2-5) were as follow

$$\dot{W} = \frac{1}{m} \cdot F_Z + Q \cdot U \quad (3-9)$$

$$\dot{Q} = \frac{1}{I_{YY}} \cdot M \quad (3-10)$$

From equations (2-35) and (2-36) the angle of attack of each foil can be written as follows:

$$\alpha_C = \frac{W_{RC}}{U} + AL_F \quad (3-11)$$

$$\alpha_S = \frac{W_{RS}}{U} + AL_S \quad (3-12)$$

$$\alpha_P = \frac{W_{RP}}{U} + AL_P \quad (3-13)$$

$$\alpha_M = \frac{W_{RM}}{U} + AL_M \quad (3-14)$$

$$W_{RP} = W + L_{YPF} \cdot P - L_{XPF} \cdot Q \quad (3-15)$$

$$W_{RS} = W + L_{YSF} \cdot P - L_{XSF} \cdot Q \quad (3-16)$$

$$W_{RM} = W + L_{XMF} \cdot Q \quad (3-17)$$

$$W_{RC} = W - L_{XCF} \cdot Q \quad (3-18)$$

Assume there is no significant coupling from the roll, yaw, sway or surge motions. Equations (3-15), (3-16), (3-17) and (3-18) will be

$$W_{RP} = W - L_{XPF} \cdot Q$$

$$W_{RS} = W - L_{XSF} \cdot Q$$

$$W_{RM} = W - L_{XMF} \cdot Q$$

$$W_{RC} = W - L_{XCF} \cdot Q$$

And equations (3-11), (3-12), (3-13) and (3-14) will be

$$\alpha_C = \frac{W}{U} - \frac{L_{XCF}}{U} \cdot Q + AL_F$$

$$\alpha_S = \frac{W}{U} - \frac{L_{XSF}}{U} \cdot Q + AL_S$$

$$\alpha_M = \frac{W}{U} - \frac{L_{XMF}}{U} \cdot Q + AL_M$$

$$\alpha_P = \frac{W}{U} - \frac{L_{XPF}}{U} \cdot Q + AL_P$$

$$L_{XSF} = L_{XPF} = L_{XMF}$$

$$\text{Let } AL_F = A_1, \quad AL_S = AL_P = AL_M = A_2$$

$$\frac{L_{XCF}}{U} \cdot Q = Q_1$$

$$\frac{L_{XSF}}{U} \cdot Q = Q_2$$

$$\frac{W}{U} = W'$$

$$\alpha_C = W' - Q_1 + A_1$$

$$\alpha_S = W' - Q_2 + A_2 = \alpha_P = \alpha_M$$

$$\text{From Equation (2-40)} \quad F_Z = F_{ZCF} + F_{ZPF} + F_{ZSF} + F_{ZMF} + F_{gZ}$$

$$F_{ZCF} = -F_{DCZ} \cdot \alpha_C - F_{LCZ} \quad (3-19)$$

$$F_{ZPF} = -F_{DPZ} \cdot \alpha_P - F_{LPZ} \quad (3-20)$$

$$F_{ZSF} = -F_{DSZ} \cdot \alpha_S - F_{LSZ} \quad (3-21)$$

$$F_{ZMF} = -F_{DMF} \cdot \alpha_M - F_{LMZ} \quad (3-22)$$

Equation (2-44) shows the general expression for hydrodynamic forces, and from Ref. 3 the linear approximation of hydrodynamic coefficients are:

$$CL_{CF} = 5.15 \alpha_C + 0.036 \delta_F + 0.13$$

$$CL_{PF} = 4.10 \alpha_P + 0.018 \delta_P$$

$$CL_{SF} = 4.10 \alpha_S + 0.018 \delta_S$$

$$CL_{MF} = 5.15 \alpha_M + 0.036 \delta_A$$

$$C_{DF} = 0.012 + 0.0015 \delta_F$$

$$C_{DA} = 0.02 + 0.0028 \delta_A$$

$$C_{DP} = 0.02 + 0.0028 \delta_P$$

$$C_{DS} = 0.02 + 0.0028 \delta_S$$

Let

$$0.5 \cdot \rho \cdot U^2 \cdot A_{CF} = D_1$$

$$0.5 \cdot \rho \cdot U^2 \cdot A_{PF} = 0.5 \cdot \rho \cdot U^2 \cdot A_{SF} = D_2$$

$$0.5 \cdot \rho \cdot U^2 \cdot A_{MF} = D_3$$

After dropping the nonlinear terms

$$F_{ZCF} = -(5.162D_1)W' + (5.162D_1)Q_1 - D_1(0.0015A_1 + 0.036)\delta_F \\ - D_1(5.162A_1 + 0.13)$$

$$F_{ZPF} = -(4.12D_2)W' + (4.12D_2)Q_2 - 4.12D_2A_2$$

$$F_{ZSF} = -(4.12D_2)W' + (4.12D_2)Q_2 - 4.12D_2A_2$$

$$F_{ZMF} = -(5.17D_3)W' + (5.17D_3)Q_2 - D_3(0.0028A_2 + 0.036)\delta_A - 5.17D_3A_2$$

$$F_Z = -(5.162D_1 + 8.24D_2 + 5.17D_3)\frac{W}{U} + (214.69D_1 - 139.92D_2 - 87.79D_3)\frac{Q}{U} \\ - D_1(0.0015A_1 + 0.036)\delta_F - D_3(0.0028A_2 + 0.036)\delta_A \\ - [D_1(5.162A_1 + 0.13) + 8.24D_2A_2 + 5.17D_3A_2]$$

$$\ddot{Z} = \frac{(5.162D_1 + 8.24D_2 + 5.17D_3)}{mU} \dot{Z} + \left[\frac{(214.69D_1 - 139.92D_2 - 87.79D_3)}{mU} \right. \\ \left. + U \right] \dot{\theta} + \frac{F_G}{m} \theta - \frac{D_1(0.0015A_1 + 0.036)}{m} \delta_F - \frac{D_3(0.0028A_2 + 0.036)}{m} \delta_A \\ - \frac{[D_1(5.162A_1 + 0.13) + 8.24D_2A_2 + 5.17D_3A_2]}{m} \quad (3-23)$$

$$M = -M_{FWD} - M_{AFT} + F_{XCF} L_{ZCF} + F_{XSF} L_{ZSF} + F_{XMF} L_{ZMF} + F_{XCS} L_{ZCS} + F_{XPS} L_{ZPS} \\ + F_{XSS} L_{ZSS} + T_X L_{ZT}$$

$$M_{FWD} = F_{ZCF} L_{XCF}$$

$$M_{AFT} = (F_{ZPF} + F_{ZSF} + F_{ZMF}) L_{XMF}$$

$$M = [(214.69D_1)W' - (214.69D_1)Q_1 + (0.212D_1A_1 + 1.497D_1)\delta_F \\ + (214.69D_1A_1 + 5.41D_1)] + [-(139.92D_2)W' + (139.92D_2)Q_2 \\ - 139.92D_2A_2 - (87.79D_3)W' + (87.79D_3)Q_2 - (0.048D_3A_2 + 0.611D_3)\delta_A \\ - 87.79D_3A_2] + [(281.1D_2A_2)W' - (281.1D_2A_2)Q_2 + (140.55D_2A_2^2 \\ - 0.686D_2)] + [(159.65D_1A_1 + 2.02D_1)W' - (159.65D_1A_1 + 2.02D_1)Q_1 \\ + (0.558D_1A_1 - 0.023D_1)\delta_F + (79.83D_1A_1^2 + 2.02A_1D_1 - 0.186)] \\ + [(176.5D_3A_2)W' - (176.5D_3A_2)Q_2 + (0.62D_3A_2 - 0.048D_3)\delta_A \\ + (88.27D_3A_2^2 - 0.343)] - 14.29U^2 + 17.7T_X$$

$$\dot{Q} = \frac{[D_1(216.71 + 159.65A_1) - D_2(139.92 - 281.1A_2) - D_3(87.79 - 179.5A_2)]}{I_{YY}} U_W \\ - \frac{[D_1(8928.96 + 6639.84A_1) + D_2(2375.84 - 4773.08A_2) + D_3(1490.67 \\ - 2996.97A_2)]}{I_{YY}} U_Q + \frac{D_1(1.474 + 0.77A_1)}{I_{YY}} \delta_F - \frac{D_3(0.659 - 0.572A_2)}{I_{YY}} \delta_A \\ + \frac{[D_1 \{5.41\{A_1(216.71 + 79.83A_1)\} - D_2\{0.686 + A_2(139.92 \\ - 140.548A_2)\} - D_3A_2(87.79 - 88.27A_2) - 0.529 - 14.29U^2 + 17.7T_X\}}{I_{YY}}$$

(3-24)

From (3-23) and (3-24)

$$\ddot{\theta} + C_2 \dot{\theta} - C_1 \dot{Z} = C_3 \delta_F - C_4 \delta_A + U_1$$

$$-C_6 \dot{\theta} - C_7 \theta + \ddot{Z} + C_5 \dot{Z} = -C_8 \delta_F - C_9 \delta_A - U_2$$

By taking the Laplace Transform of the two equations above and rearranging into a matrix form

$$\begin{bmatrix} S(S+C_2) & -C_1 S \\ -(C_6 S+C_7) & S(S+C_5) \end{bmatrix} \begin{bmatrix} \theta \\ Z \end{bmatrix} = \begin{bmatrix} C_3 & -C_4 \\ -C_8 & -C_9 \end{bmatrix} \begin{bmatrix} \delta_F \\ \delta_A \end{bmatrix} + \begin{bmatrix} U_1 \\ -U_2 \end{bmatrix}$$

The characteristic equation

$$\Delta = S[S\{S^2+(C_2+C_5)\}-C_1C_6S-C_1C_7]$$

where:

$$C_1 = \frac{[D_1(216.71 - 139.65A_1) - D_2(139.92 - 281.1A_2) - D_3(87.79 - 176.5A_2)]}{I_{YY} U}$$

$$C_2 = \frac{[D_2(8928.96 + 6639.84A_1) + D_2(2375.84 - 4773.08A_2) + D_3(1490.67 - 2996.97A_2)]}{I_{YY} U}$$

$$C_3 = \frac{[D_1(1.474 + 0.77A_1)]}{I_{YY}}$$

$$C_4 = \frac{[D_3(0.659 - 0.572A_2)]}{I_{YY}}$$

$$C_5 = \frac{[5.162D_1 + 8.24D_2 + 5.17D_3]}{mU}$$

$$C_6 = \frac{[(214.69D_1 - 139.92D_2 - 87.79D_3) + U]}{mU}$$

$$C_7 = \frac{F_G}{m}$$

$$C_8 = \frac{[D_1(0.0015A_1+0.036)]}{m}$$

After inserting the value of parameters, a speed of 36 knots was chosen to be used in this simulation to insure that cavitation did not exist, and it was assumed that there was no external disturbance. The transfer function matrix becomes:

$$\begin{bmatrix} S(S+10.791) & -0.063S \\ -(76.33S+32.2) & S(S+7.61) \end{bmatrix} \begin{bmatrix} \theta \\ Z \end{bmatrix} = \begin{bmatrix} 0.083 & -0.0394 \\ -1.04 & -1.215 \end{bmatrix} \begin{bmatrix} \delta_F \\ \delta_A \end{bmatrix}$$

and the characteristic equation was

$$\begin{aligned} \Delta &= S[S^3+18.4S^2+77.31S-2.03] \\ &= S(S-0.0261)(S+6.55)(S+11.876) \end{aligned}$$

and

$$\left. \frac{\theta}{\delta_F} \right|_{\delta_A=0} = \frac{\begin{vmatrix} 0.083 & -0.063S \\ -1.04 & S(S+7.61) \end{vmatrix}}{\Delta} = \frac{0.083(S+6.82)}{(S+0.0261)(S+6.55)(S+11.876)}$$

$$\left. \frac{-Z}{\delta_F} \right|_{\delta_A=0} = \frac{\begin{vmatrix} S(S+10.731) & 0.083 \\ (76.33S+32.2) & 1.04 \end{vmatrix}}{\Delta} = \frac{1.04(S-0.495)(S+5.19)}{S(S-0.0261)(S+6.55)(S+11.876)}$$

$$\left. \frac{\theta}{\delta_A} \right|_{\delta_F=0} = \frac{\begin{vmatrix} -0.0394 & -0.063S \\ -1.215 & S(S+7.61) \end{vmatrix}}{\Delta} = \frac{-0.0394(S+9.55)}{(S-0.0261)(S+6.55)(S+11.876)}$$

$$\left. \frac{-Z}{\delta_A} \right|_{\delta_F=0} = \frac{\begin{vmatrix} S(S+10.791) & 0.0394 \\ -(76.33S+32.2) & 1.215 \end{vmatrix}}{\Delta} = \frac{1.215(S+0.079)(S+13.186)}{S(S-0.0261)(S+6.55)(S+11.876)}$$

$$W_E = -U \sin \theta + V \cos \theta \sin \phi + W \cos \theta \cos \phi$$

V, the velocity in Y-direction is equal to zero, and angle θ is assumed small.

$$\sin \theta = \theta, \quad \cos \theta = 1.$$

$$W_E = -U \cdot \theta + W$$

$$-h_{cg} = -Z_E = -\left(\frac{W}{S} - \frac{U}{S} \cdot \theta\right)$$

The height at the sensor,

$$-h_S = -h_{cg} + L_{XH} \cdot \theta$$

$$-h_S = -\frac{W}{S} + \frac{W}{S} \cdot \theta + L_{XH} \cdot \theta$$

$$\left. \frac{-h_S}{\delta_F} \right|_{\delta_A=0} = \left. \frac{-Z}{\delta_F} \right|_{\delta_Z=0} + \frac{U}{S} \left. \frac{\theta}{\delta_F} \right|_{\delta_A=0} + L_{XH} \left. \frac{\theta}{\delta_F} \right|_{\delta_A=0}$$

$$\left. \frac{-h_S}{\delta_A} \right|_{\delta_F=0} = \left. \frac{-Z}{\delta_A} \right|_{\delta_F=0} + \frac{U}{S} \left. \frac{\theta}{\delta_A} \right|_{\delta_F=0} + L_{XH} \left. \frac{\theta}{\delta_A} \right|_{\delta_F=0}$$

The four transfer functions of the craft are:

$$\left. \frac{\theta}{\delta_F} \right|_{\delta_A=0} = \frac{0.083(S+6.82)}{(S-0.0261)(S+6.55)(S+11.876)}$$

$$\left. \frac{-h_S}{\delta_F} \right|_{\delta_A=0} = \frac{6.68(S+0.72)(S+6.52)}{S(S-0.0261)(S+6.55)(S+11.876)}$$

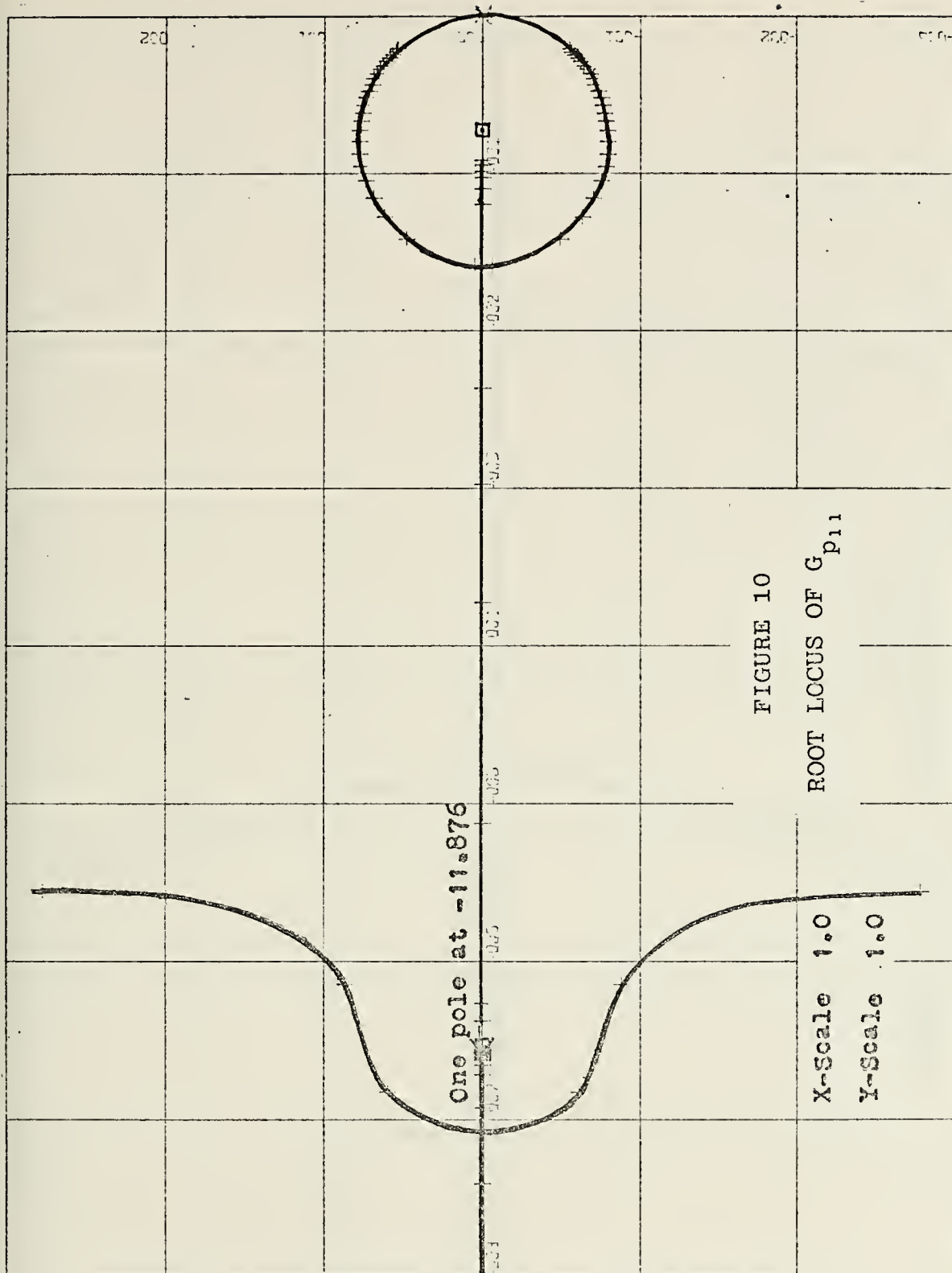
$$\left. \frac{\theta}{\delta_A} \right|_{\delta_F=0} = \frac{-0.0394(S+9.55)}{(S-0.0261)(S+6.55)(S+11.876)}$$

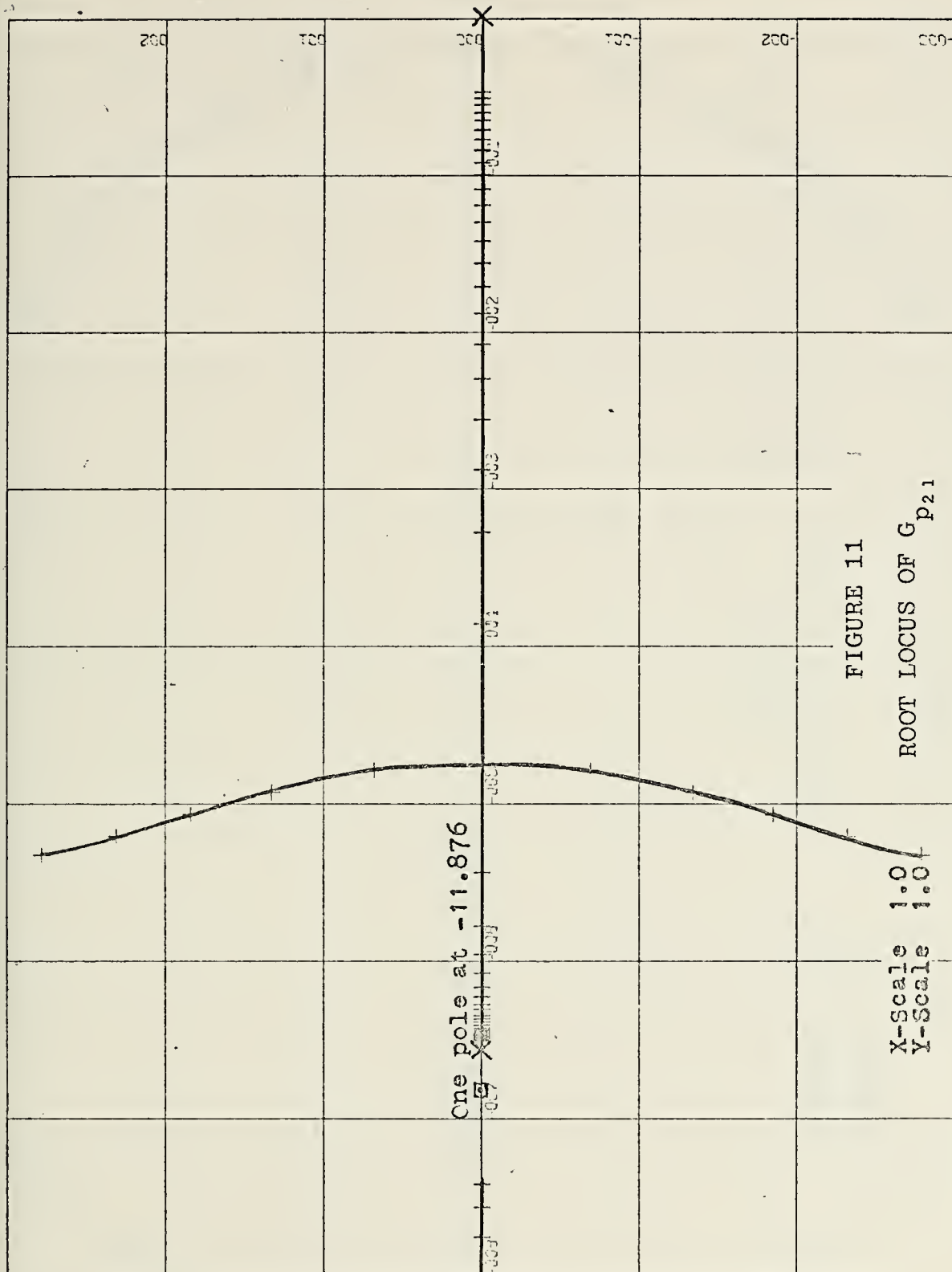
$$\left. \frac{-h_S}{\delta_A} \right|_{\delta_F=0} = \frac{-1.464(S+2.72)(S+5.348)}{S(S-0.0261)(S+6.55)(S+11.876)}$$

The characteristic equation shows that this system has one pole in the right half plane, and from the Root Locus plots three of the plant transfer functions have roots in right half plane, only the effect of forward foil to the height sensor has complex roots in the left half plane but very close to the imaginary axis, which was only marginally stable. From this point, the stability of the craft without automatic control system was questioned, and led to the conclusion that the craft must have an automatic control system.

B. ROOT LOCUS DESIGN OF FORWARD FOIL AUTOMATIC CONTROL

Considering only the forward foil as a control surface, the aft foil was fixed at the angle of 0.074269 radian [Ref. 1]. By closing the height loop and the pitch angle loop as in Figure 14 and increasing gain K of the system to 5, from







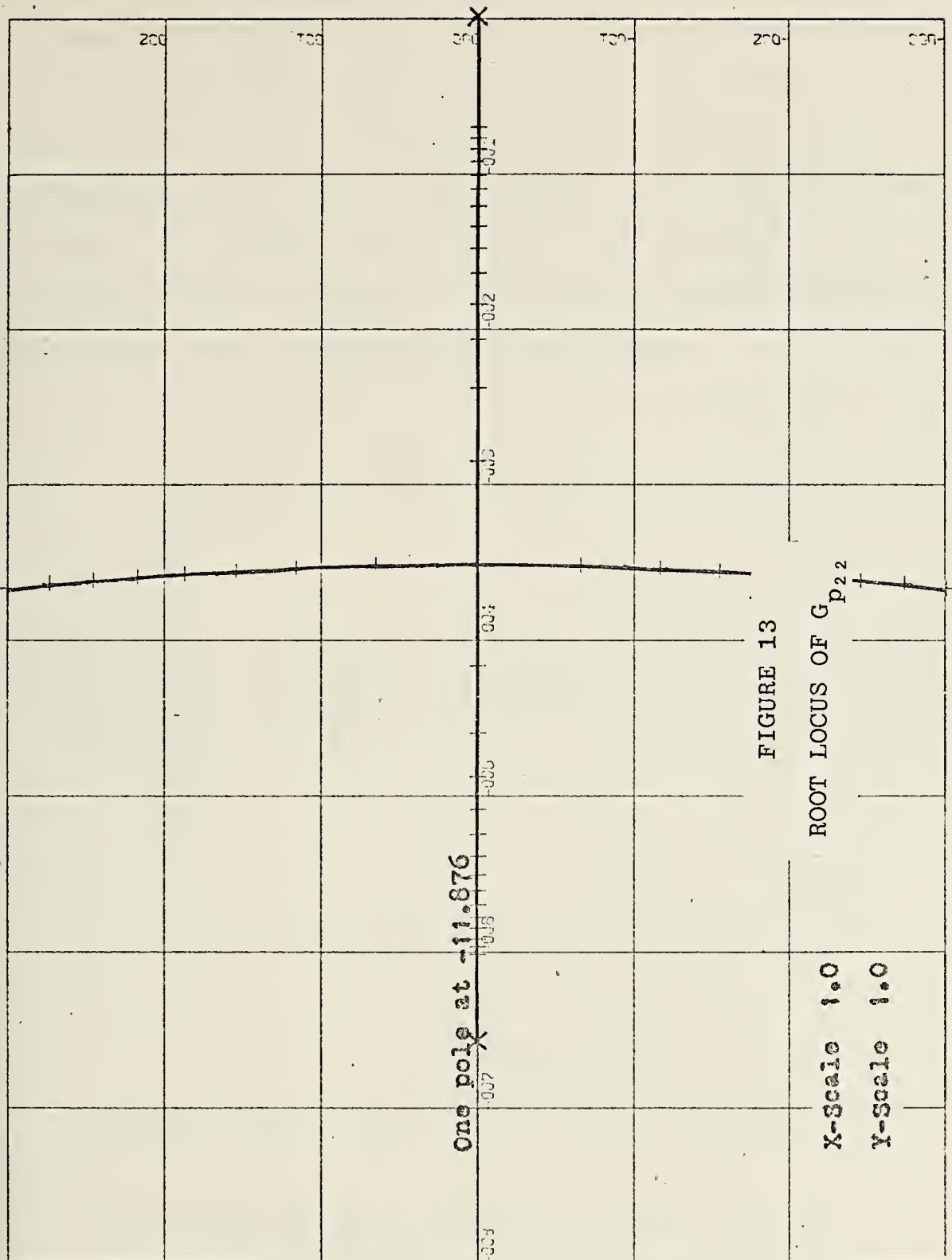


Figure 10 the roots of the height loop moved further into the left half plane and became repeated real roots at -1.6 . This value of gain K pushes the root of the pitch angle loop (Figure 11) just across the imaginary axis to the left half plane. The system becomes stable. The response to the change in height command of 2.0 feet was shown in Figure 15. The craft went to steady state in 5.5 sec.

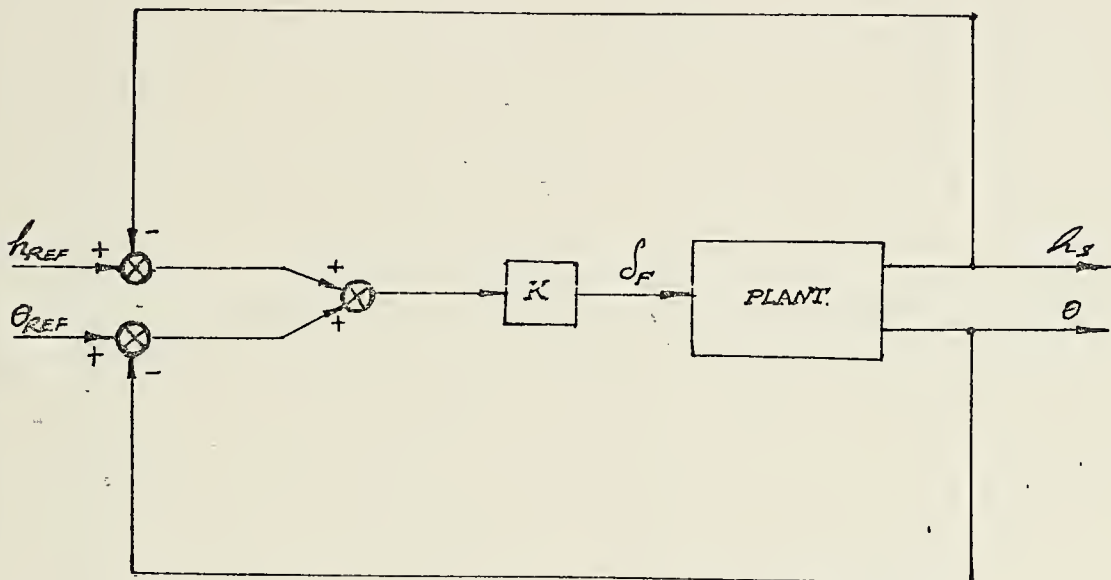
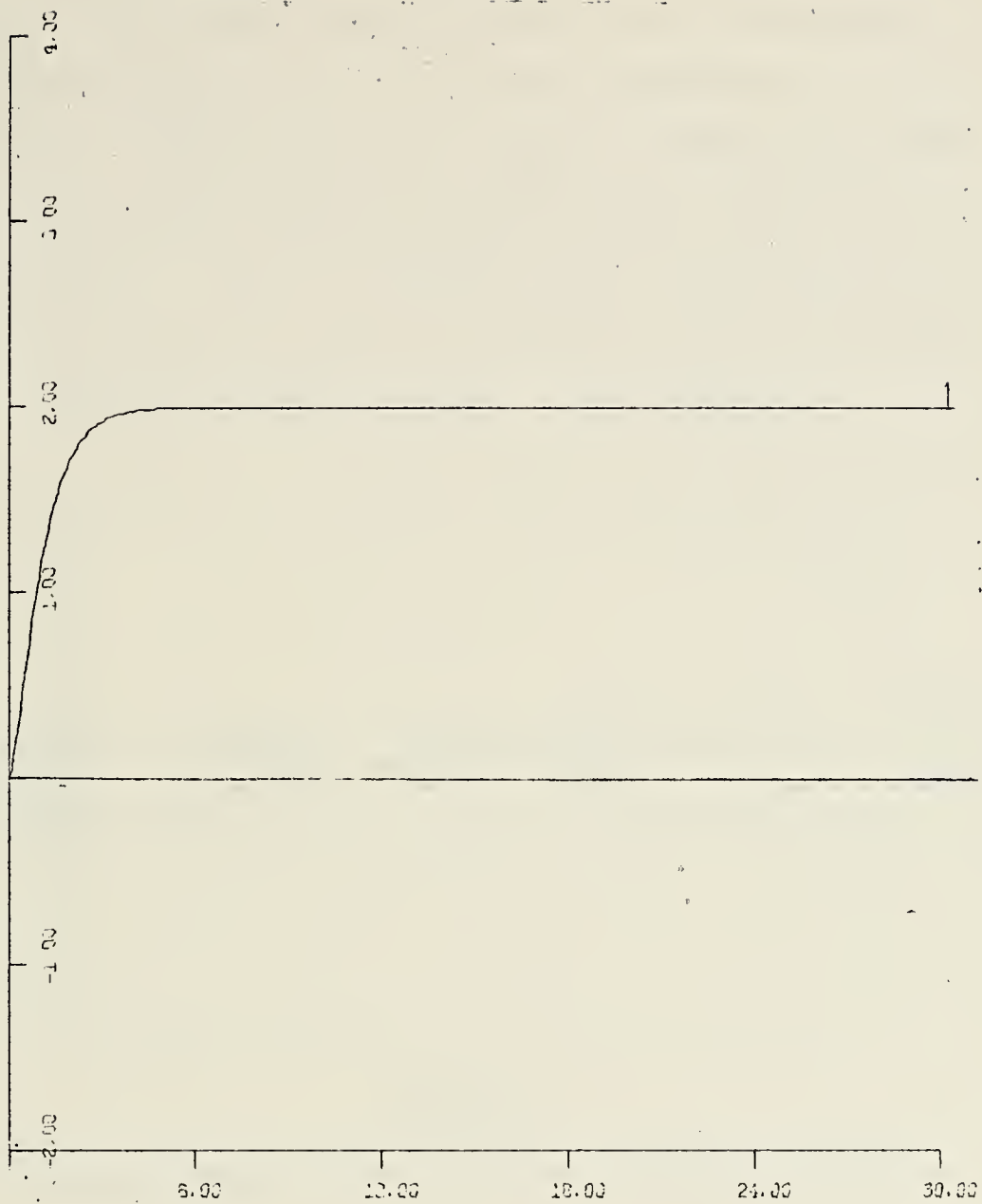


FIGURE 14

BLOCK DIAGRAM SHOWING FORWARD FOIL AUTOMATIC CONTROL

C. ROOT LOCUS DESIGN OF AFT FOIL AUTOMATIC CONTROL

In like manner, if the aft foil is used as a control surface and the forward foil is fixed at the angle of 0.03711 radian, the system is unstable by itself, because



X-Scale 6.0

Y-Scale 1.0

FIGURE 15
STEP RESPONSE OF THE CRAFT
(FORWARD FOIL ONLY)

the open loop roots of both height and pitch angle were in the right half plane. From the Root Locus plots Figures 12, 13, positive gain will have the roots further into the right half plane. After closing the loops and using gain K equal to -47 , the height loop had complex roots at $-3 \pm j3$. The right half plane root of the pitch angle loop moved toward the left half plane, across the imaginary axis to the point -0.2 . The system becomes stable. (See Figure 16.)

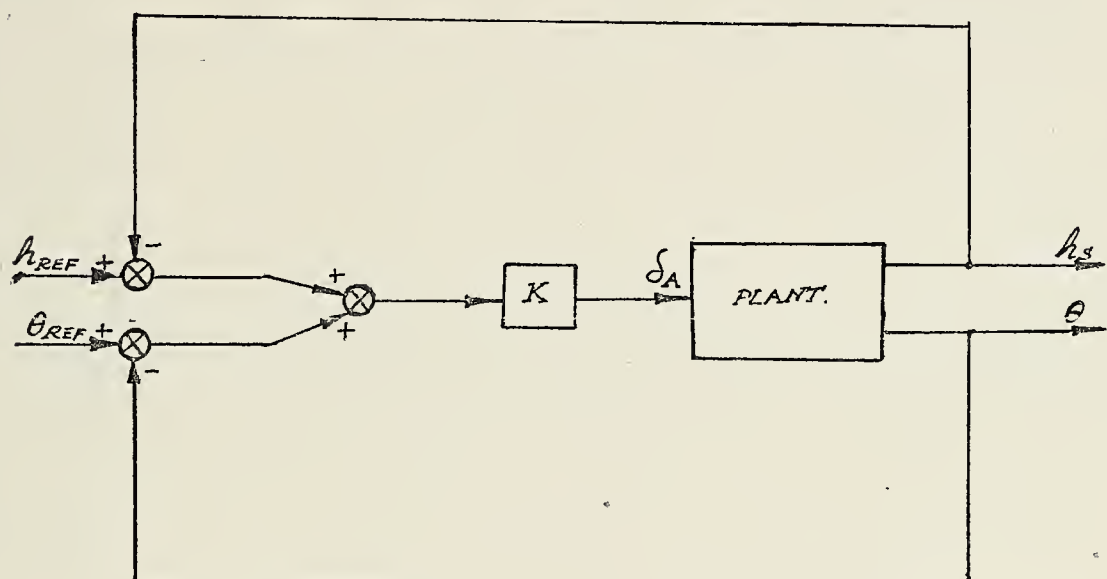


FIGURE 16

BLOCK DIAGRAM SHOWING AFT FOIL AUTOMATIC CONTROL

Figure 17 shows the response of the craft to the change in height command of two feet. Because the flap angle was limited at $\pm 5^\circ$, and the gain of the aft foil was too high, in the first five seconds the flap exceeded its limit and the flap angle was set to 5° which had the same result as reducing the gain of the system. Then in the first five

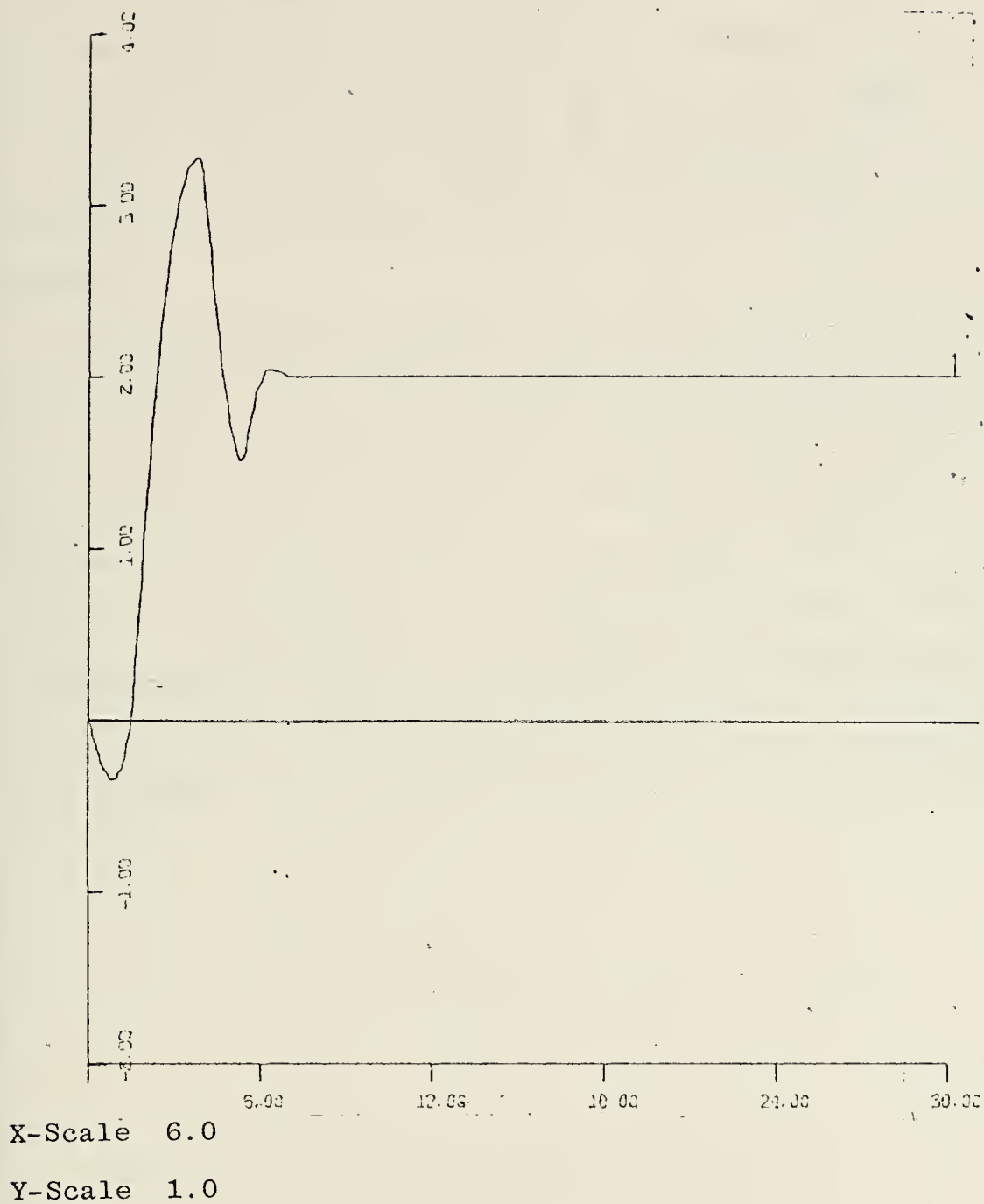


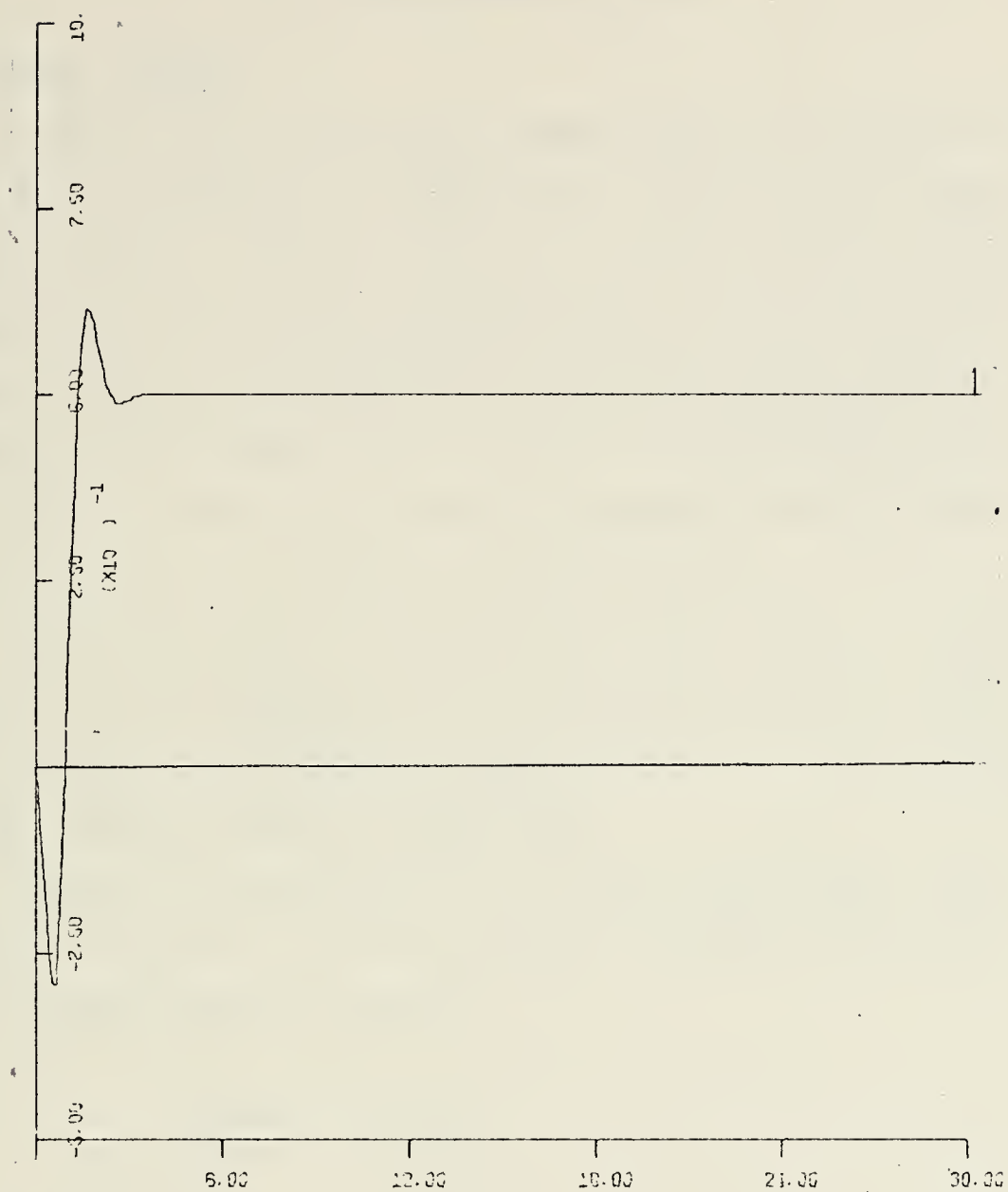
FIGURE 17

STEP RESPONSE OF THE CRAFT

(AFT. FOIL ONLY, INPUT = 2.0)

seconds the craft behaved like a very lightly damped system, but after five seconds the craft became more stable and reached steady state in eight seconds. Figure 18 shows the response of the craft when the change in height command was 0.5 foot. In the first 1.0 sec. the flap angle still exceeded the limit, but the craft went to steady state in 3.0 seconds.

Parts B and C have shown that the stability of the craft in pitch-heave mode can be achieved by using either forward or aft foil as a control surface with the other foil fixed. But to make the craft completely stable in six degrees of freedom both forward and aft foil have to be used as control surfaces. The dynamics of the system will produce a cross coupling effect between the two inputs, the systems now have multiple inputs and multiple outputs, which is a classical multivariable system and will be studied in the next chapter.



X-Scale 6.0

Y-Scale 0.25

FIGURE 18
STEP RESPONSE OF THE CRAFT
(AFT. FOIL ONLY, INPUT = 0.5)

V. MULTIVARIABLE SYSTEM

A. BASIC CONCEPT

A system which has multiple inputs-multiple outputs is much more complicated to design than a single input-single output system, because a change in one input may have an effect not only on the corresponding output but also on the other outputs. In designing this kind of system, special techniques are needed. Ref. 9 has all of the theories and procedures to work on this kind of problem, and this paper will follow the procedures in that reference.

The idea was that, the plant has a $n \times m$ transfer function matrix and was compensated by a $m \times n$ diagonal matrix compensator with unity feedback. The configuration of the compensated system is shown in Figure 19.

Consider the hydrofoil craft in pitch-heave mode only, and not coupled to the other modes. The craft will have a 2×2 transfer function matrix.

$$G_p = \begin{bmatrix} g_{p_{11}} & g_{p_{12}} \\ g_{p_{21}} & g_{p_{22}} \end{bmatrix} \quad (4-1)$$

If the diagonal compensator matrix

$$G_c = \begin{bmatrix} g_{c_{11}} & 0 \\ 0 & g_{c_{22}} \end{bmatrix} \quad (4-2)$$

is used, the system configuration becomes

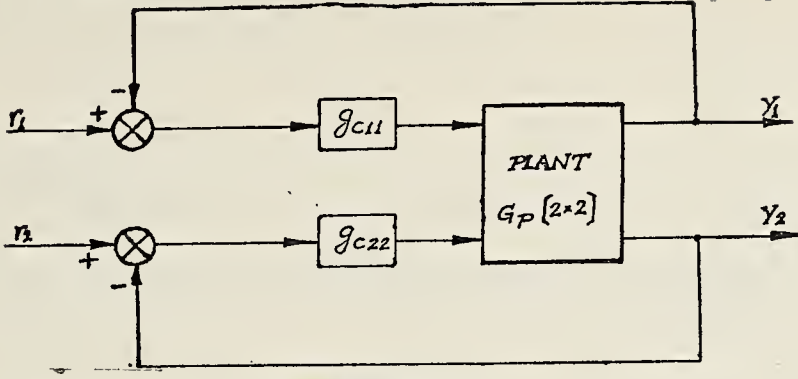


FIGURE 19

BLOCK DIAGRAM SHOWING A MULTIVARIABLE SYSTEM
WITH DIAGONAL MATRIX CASCADE COMPENSATOR

$$G_p G_c = \begin{bmatrix} g_{p11} g_{c11} & g_{p12} g_{c22} \\ g_{p21} g_{c11} & g_{p22} g_{c22} \end{bmatrix} \quad (4-3)$$

1. The Characteristic Equation

The stability of a multivariable system is determined by the zeros of $N_1(s)$ and $N(s)$, which are defined as follows:

$$\frac{N_1(s)}{D_1(s)} \triangleq \det [I + G_p(s) G_c(s)] \quad (4-4)$$

$$\hat{N}(s) \triangleq \frac{\Delta_c(s) \cdot \Delta_p(s)}{D_1(s)} \quad (4-5)$$

and $\Delta_c(s)$, $\Delta_p(s)$ represent the characteristic polynomials of the rational transfer function matrices $G_c(s)$ and $G_p(s)$, respectively.

If

- 1) Cancellations are selected systematically, as in Ref. 9,

2) Poles of G_c are carefully selected,
then (4-4) alone determines the stability of the system.
Thus

$$\det(I + G_p G_c) = 0$$

will be referred to as the characteristic equation of multi-variable system.

2. Connection Between Single-Loop and Multivariable

Cases for 2×2 Plant G_p , and 2×2 Diagonal G_c

$$\begin{aligned} \det(I + G_p G_c) &= 1 + g_{p_{11}} g_{c_{11}} + g_{p_{22}} g_{c_{22}} + (\det \cdot G_p) g_{c_{11}} g_{c_{22}} \\ &= (1 + g_{p_{11}} g_{c_{11}}) \left(1 + \frac{g_{p_{22}} + (\det \cdot G_p) g_{c_{11}}}{1 + g_{p_{11}} g_{c_{11}}} g_{c_{22}} \right) \end{aligned} \quad (4-6)$$

$$= (1 + g_{p_{11}} g_{c_{11}}) (1 + G_{eq} g_{c_{22}}) \quad (4-7)$$

where

$$G_{eq} = \frac{g_{p_{22}} + (\det \cdot G_p) g_{c_{11}}}{1 + g_{p_{11}} g_{c_{11}}} = \frac{g_{p_{22}} \left(1 + \frac{\det \cdot G_p}{g_{p_{22}}} g_{c_{11}} \right)}{1 + g_{p_{11}} g_{c_{11}}}$$

The roots of the characteristic equation are the zeros of the rational function $(1 + g_{p_{11}} g_{c_{11}}) (1 + G_{eq} g_{c_{22}})$.

From (4-6), can be seen that the roots of

$$1 + \frac{\det \cdot G_p}{g_{p_{22}}} g_{c_{11}} = 0 \quad (4-8)$$

and

$$1 + g_{p_{11}} g_{c_{11}} = 0 \quad (4-9)$$

constitute part of the zeros and poles of G_{eq} , respectively and $\frac{\det \cdot G}{g_{p_{22}}}$ and $g_{p_{11}}$ are known functions.

Therefore, any single-loop method can be used in designing $g_{c_{11}}$ to place the roots of (4-8) and (4-9) at desirable locations, and also has to form a reasonably good pole-zero pattern for G_{eq} . After $g_{c_{11}}$ is designed, all poles and zeros of G_{eq} are known and $g_{c_{22}}$ can be designed from

$$1 + G_{eq} g_{c_{22}} = 0 \quad (4-10)$$

B. ROOT LOCUS DESIGN FOR PITCH-HEAVE MODE

From the craft transfer function matrix

$$G_p = \begin{bmatrix} \frac{-h_S}{\delta_F} & \frac{-h_S}{\delta_A} \\ \frac{\theta}{\delta_F} & \frac{\theta}{\delta_A} \end{bmatrix}$$

$$g_{p_{11}} = \frac{-h_S}{\delta_F} = \frac{6.68(S+0.72)(5+6.52)}{S(S-0.0261)(S+6.55)(S+11.876)}$$

$$g_{p_{12}} = \frac{-h_S}{\delta_A} = \frac{-1.464(S+2.72)(S+5.348)}{S(S-0.0261)(S+6.55)(S+11.876)}$$

$$g_{p_{21}} = \frac{\theta}{\delta_F} = \frac{0.083(S+6.82)}{(S-0.0261)(S+6.55)(S+11.876)}$$

$$g_{p_{22}} = \frac{\theta}{\delta_A} = \frac{-0.0394(S+9.55)}{(S-0.0261)(S+6.55)(S+11.876)}$$

$$\begin{aligned}\det \cdot G_p &= g_{p_{11}} g_{p_{22}} - g_{p_{12}} g_{p_{21}} \\ &= \frac{-0.141(S-0.02325)(S+6.51)(S+12.02)}{S(S-0.0261)^2(S+6.55)^2(S+11.876)^2}\end{aligned}$$

$$\frac{\det \cdot G_p}{g_{p_{22}}} = \frac{3.579(S-0.02325)(S+6.51)(S+12.02)}{S(S-0.0261)(S+6.55)(S+11.876)}$$

The design procedure starting from $g_{c_{11}}$, by plotting the root locus of equations (4-8) and (4-9) as in Figures 20 and 21, from Figure 20 can be seen that, as the gain was increased the root in the right half plane moved toward the left half plane, met pole at the origin, broke away and circled around the zero at -0.72, with the value of the gain equal to 5. Two dominant roots were at -1.25 and -2.2, and other two roots at -6.75 and -11.45 and the effect of this gain pushes the right half plane root of equation (4-8) to the left and was cancelled by the zero at +0.02325 as in Figure 21, the pole at the origin moved further into the left half plane to the point -2.3 and the other roots were in the left half plane at $-6.8 \pm j0.8$ and -11.99. Therefore, by using the gain equal to 5 as $g_{c_{11}}$, the height loop was stabilized and, this also gave a good pole-zero pattern for G_{eq} .

Equations (6-30) - (6-35) of Ref. 9 show the procedures to find poles and zeros of G_{eq} , which were listed below

$$G_1 = 1 + g_{p_{11}} g_{c_{11}} \quad (4-11)$$

$$G_2 = g_{p_{22}} + (\det \cdot G_p) g_{c_{11}} \quad (4-12)$$

One pole at -11.876

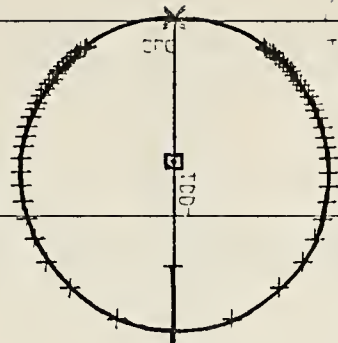


FIGURE 20

ROOT LOCUS OF $1+G_{p11} \cdot G_{c11}$

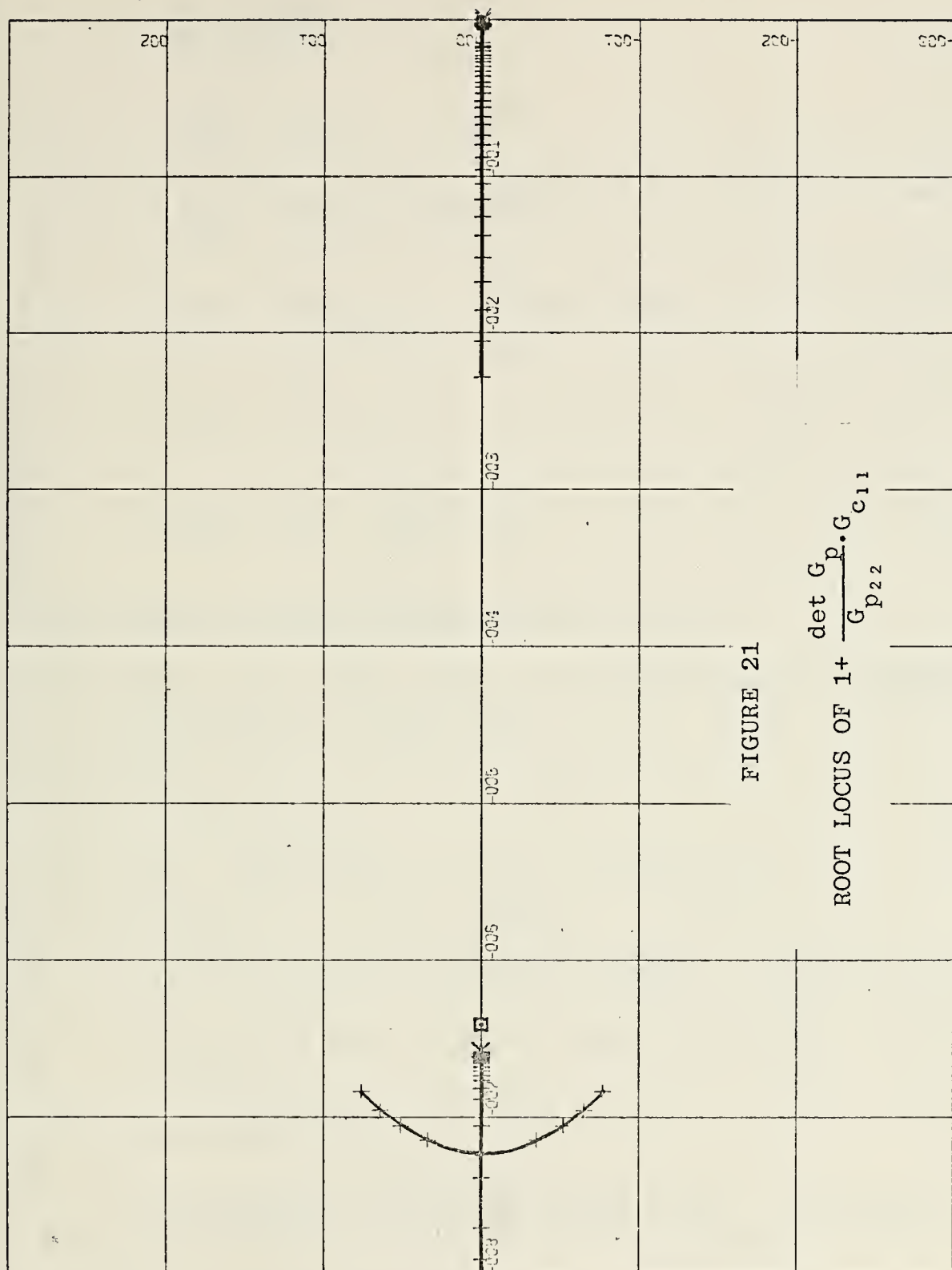


FIGURE 21

$$\text{ROOT LOCUS OF } 1 + \frac{\det G_p \cdot G_{c11}}{G_{p22}}$$

$$G_{eq} = \frac{G_2}{G_1} \quad (4-13)$$

$$P_{G_{eq}} = Z_{G_1} + P_{G_2} - (P_{G_2} \cap P_{G_1}) \quad (4-14)$$

$$Z_{G_{eq}} = Z_{G_2} + P_{G_1} - (P_{G_2} \cap P_{G_1}) \quad (4-15)$$

$$P_{G_1} = P_{g_{p_{11}} g_{c_{11}}} = P_{g_{p_{11}}} + P_{g_{c_{11}}} \quad (4-16)$$

$$Z_{G_1} = Z_1 + g_{p_{11}} g_{c_{11}} \quad (4-17)$$

$$Z_{G_2} = Z_1 + \frac{\det \cdot G_p}{g_{p_{22}}} g_{c_{11}} \quad (4-18)$$

And from the system transfer function matrix

$$P_{G_1} = P_{g_{p_{11}}} P_{g_{c_{11}}} = P_{g_{p_{11}}} + P_{g_{c_{11}}} = \{0, 0.0261, -6.55, -11.876\} + P_{g_{c_{11}}}$$

$$Z_{G_1} = Z_1 + g_{p_{11}} g_{c_{11}}$$

$$\begin{aligned} P_{G_2} &= P_{g_{p_{22}}} + P(\det \cdot G_p) g_{c_{11}} - [P_{g_{p_{22}}} \cap P(\det \cdot G_p) g_{c_{11}}] \\ &= \{0.0261, -6.55, -11.876\} + \{0, (0.0261)^2, (-6.55)^2, (-11.876)^2\} \\ &\quad + P_{g_{c_{11}}} - [\{0.0261, -6.55, -11.876\} \cap \{0, (0.0261)^2, (-6.55)^2, \\ &\quad (-11.876)^2\} + g_{c_{11}}] \\ &= \{0, (0.0261)^3, (-6.55)^3, (-11.876)^3\} + P_{g_{c_{11}}} - [\{(0.0261), \\ &\quad (-6.55), (-11.876)\}] \end{aligned}$$

$$= \{0, (0.0261)^2, (-6.55)^2, (-11.876)^2\} + P_{g_{c_{11}}}$$

$$Z_{G_2} = Z_1 + \frac{\det \cdot G_p}{g_{p_{22}}} g_{c_{11}}$$

$$P_{G_1} \cap P_{G_2} = \{0, 0.0261, -6.55, -11.876\} + P_{g_{c_{11}}} = P_{G_1}$$

$$P_{G_{eq}} = Z_1 + g_{p_{11}} g_{c_{11}} + \{0, (0.0261)^2, (-6.55)^2, (-11.876)^2\} + P_{g_{c_{11}}}$$

$$- \{0, 0.0261, -6.55, -11.376\} - P_{g_{c_{11}}}$$

$$= Z_1 + g_{p_{11}} g_{c_{11}} + \{(0.0261), (-6.55), (-11.876)\}$$

$$Z_{G_{eq}} = Z_{G_2} = Z_1 + \frac{\det \cdot G_p}{g_{p_{22}}} g_{c_{11}}$$

G_{eq} has three known poles at 0.0261, -6.55, -11.876; the other poles were the roots of equation (4-9)

$$1 + g_{p_{11}} g_{c_{11}} = 0$$

The zeros of G_{eq} were the roots of equation (4-8)

$$1 + \frac{\det \cdot G_p}{g_{p_{22}}} g_{c_{11}} = 0$$

and therefore

$$G_{eq} = \frac{K_{eq} (S+2.3)(S+6.8 \pm j0.8)(S+11.99)}{(S-0.0261)(S+1.25)(S+2.2)(S+6.55)(S+6.75)(S+11.45)(S+11.876)}$$

and from

$$G_{eq} = \frac{g_{p_{22}} + (\det \cdot G_p) g_{c_{11}}}{1 + g_{p_{11}} g_{c_{11}}}$$

$$= \frac{\frac{0.0394(S+9.55)}{(S-0.0261)(S+6.55)(S+11.876)} - \frac{0.144(S-0.02325)(S+6.51)(S+12.02)}{S(S-0.0261)^2(S+6.55)^2(S+11.876)^2}}{1 + \frac{6.68(S+0.72)(S+6.52)}{S(S-0.0261)(S+6.55)(S+11.876)}}$$

$$= \frac{-0.0394(S+Z_1)(S+Z_2)-----}{(S+P_1)(S+P_2)-----}$$

$$K_{eq} = -0.0394$$

(4-19)

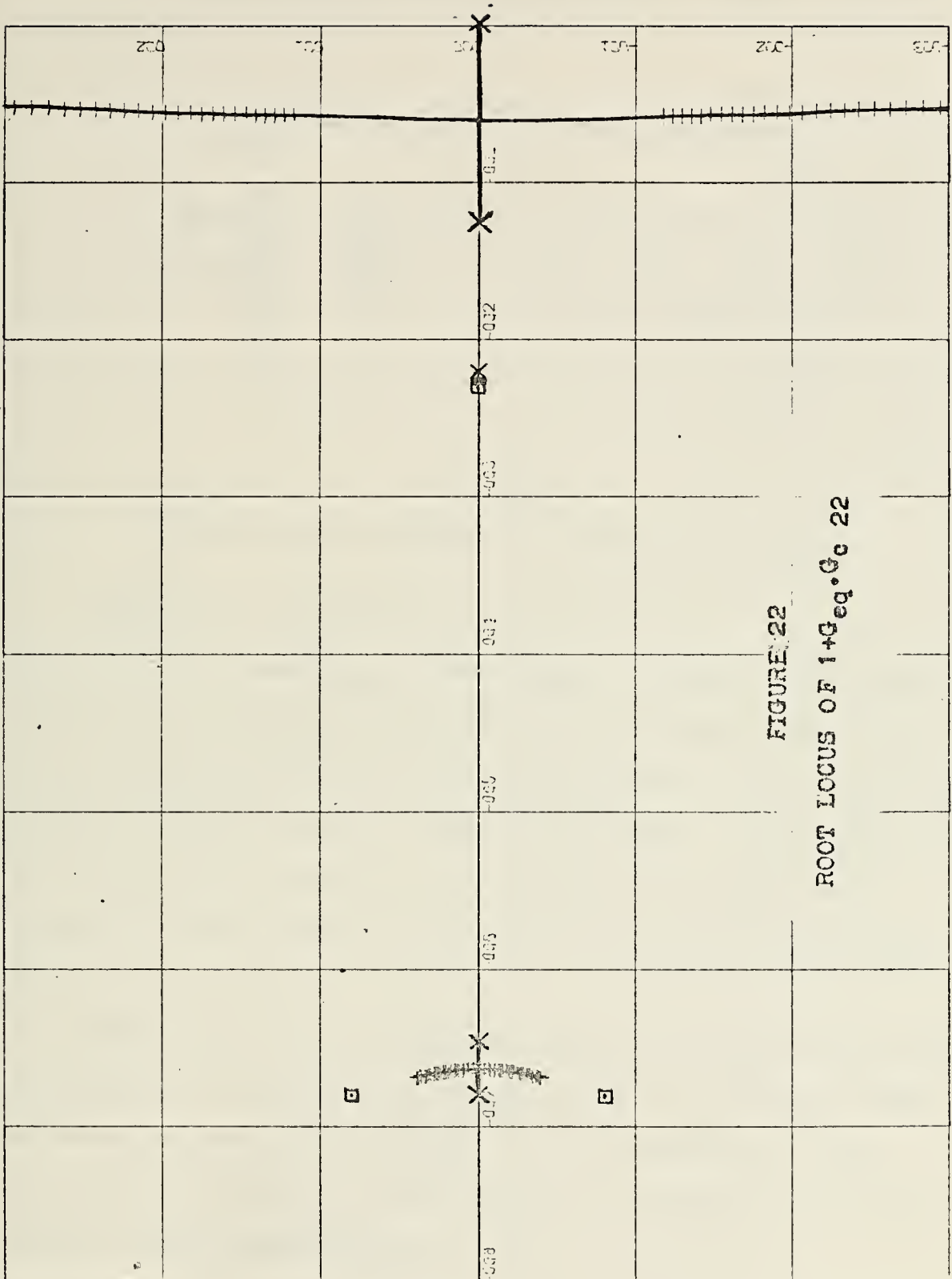
$$G_{eq} = \frac{-0.0394(S+2.3)(S+6.8 \pm j0.8)(S+11.99)}{(S-0.0261)(S+1.25)(S+2.2)(S+6.55)(S+6.75)(S+11.65)(S+11.876)}$$

Equations (4-10) and (4-19) were the equations used in designing the compensator $g_{p_{22}}$.

Figure 22 is the root locus plot for designing $g_{p_{22}}$. The positive gain will push the pole at 0.0261 further into the right half plane; therefore positive gain cannot be used to compensate this system. Negative gain which can make the gain of the system equal to 3.881 will set dominant roots at $-0.7 \pm j0.2$, which is a pretty good position. Therefore, using the gain of the system equal to 3.881, we can make system stable and the pitch angle loop has good damping. The compensator $g_{p_{22}}$ thus becomes a pure gain of value

$$K_2 K_{eq} = 3.881$$

$$K_2 = \frac{3.881}{-0.0396} = -98$$



The configuration of the compensated system is shown in Figure 23.

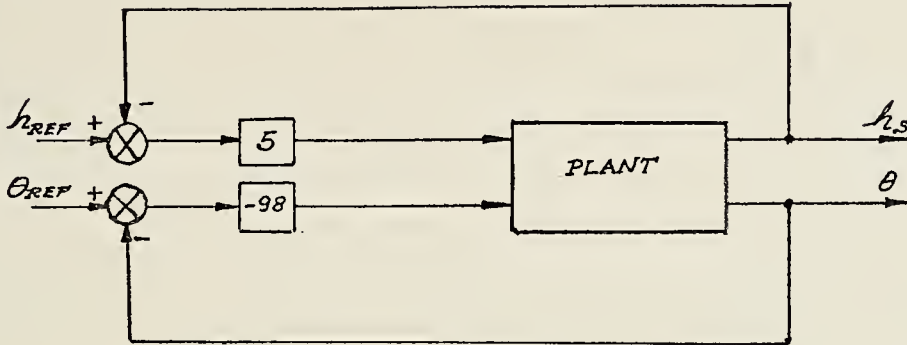
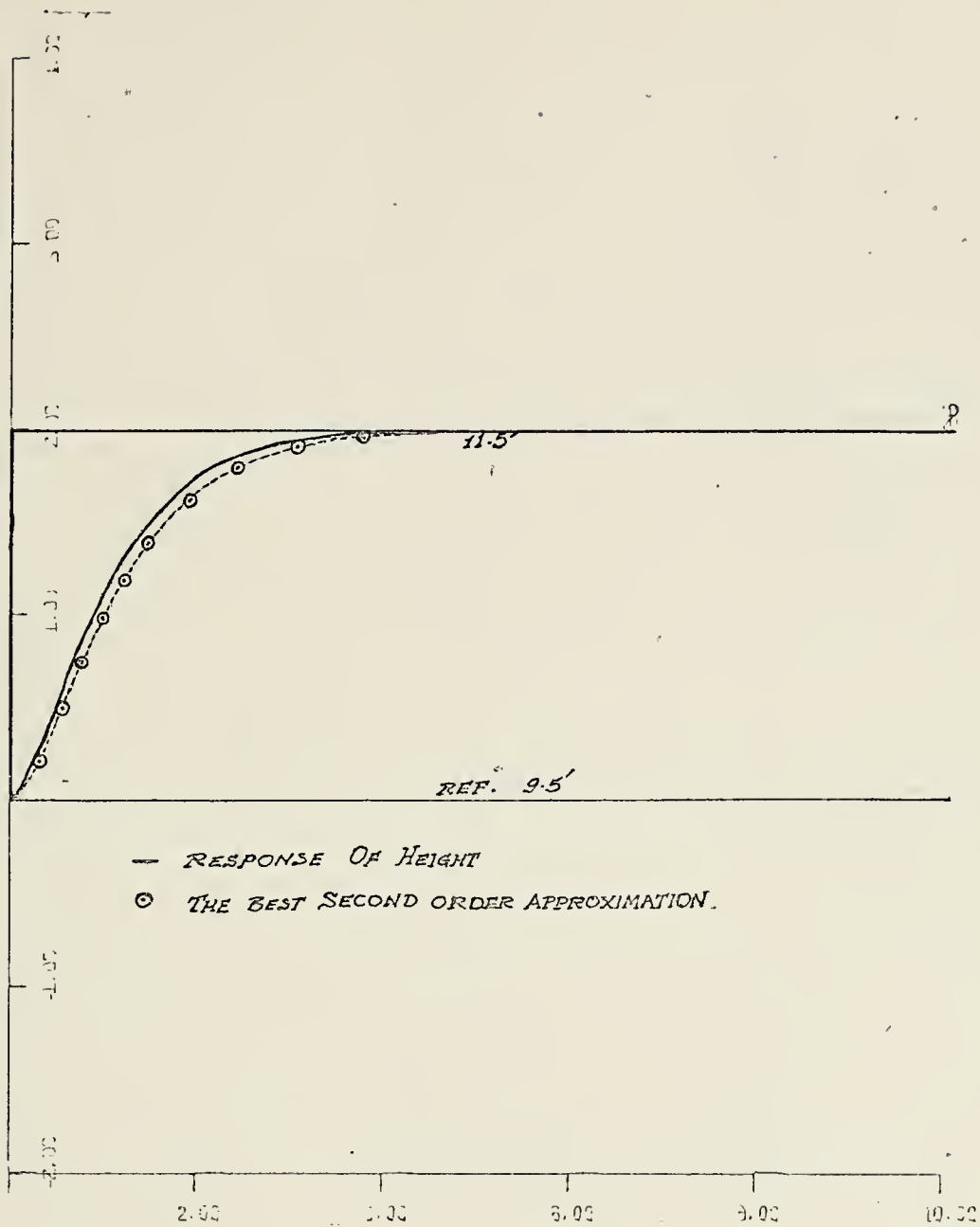


FIGURE 23

BLOCK DIAGRAM SHOWING THE COMPENSATED SYSTEM

Referring to Figure 20, the dominant roots were at -1.25 and -2.2 which gave $\omega_n = 1.658$, and $\zeta = 1.04$. Figure 24 shows the response of the craft when the height above the water has changed from 9.5 feet to 11.5 feet, and Figure 25, when it changes from 11.5 feet to 9.5 feet. The response of the craft was the same in both cases and followed very closely to the response of the best second order approximation.

Figure 26 is the response of the pitch angle from 2° bow up back to 0° reference and Figure 27 is the response from 2° stern up back to 0° reference. The response in both cases was the same but faster than the response of the best second order approximation.



X-Scale 2.0

Y-Scale 1.0

FIGURE 24
STEP RESPONSE OF HEIGHT (2 FT. UP)

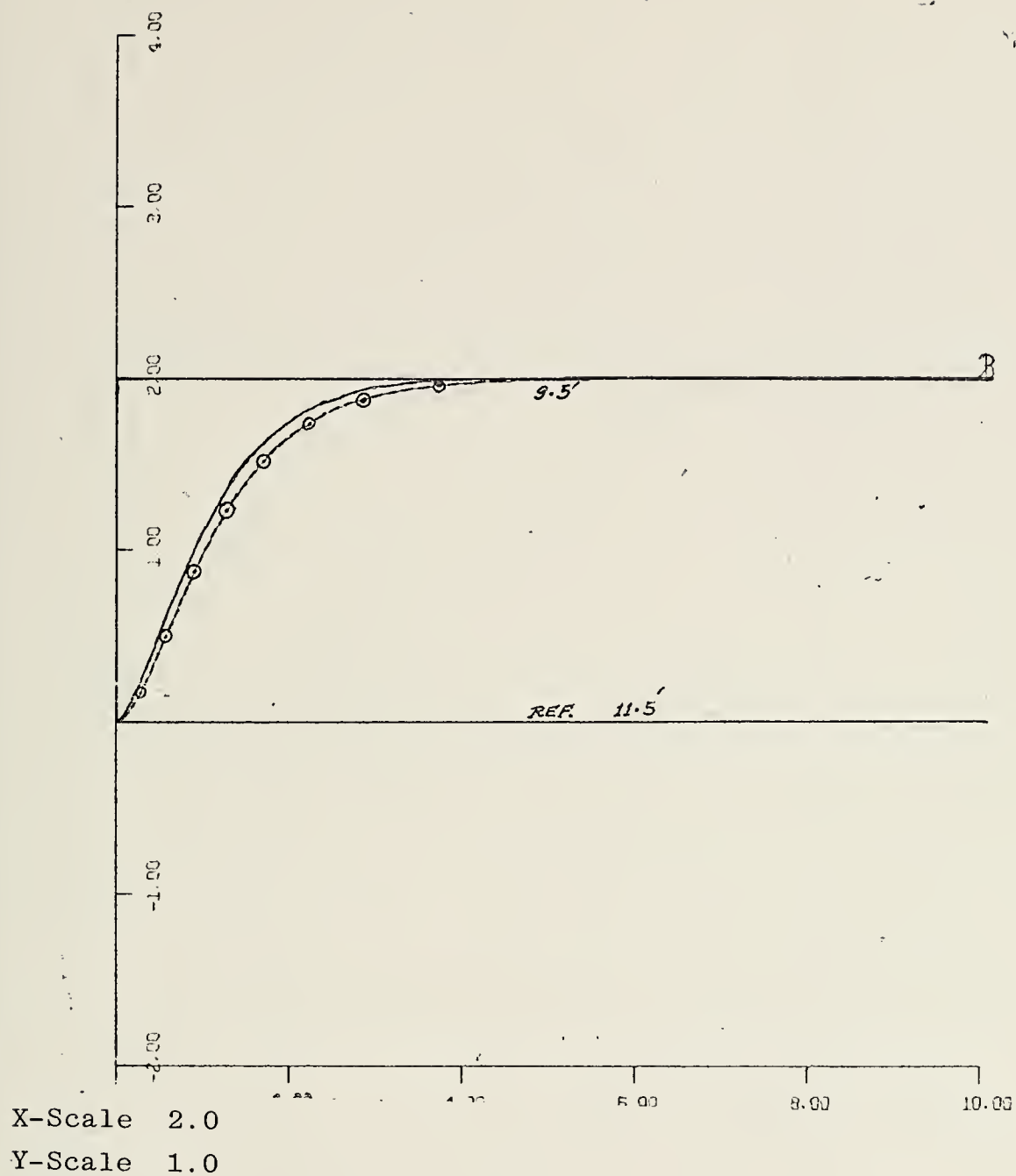


FIGURE 25
STEP RESPONSE OF HEIGHT (2 FT. DOWN)

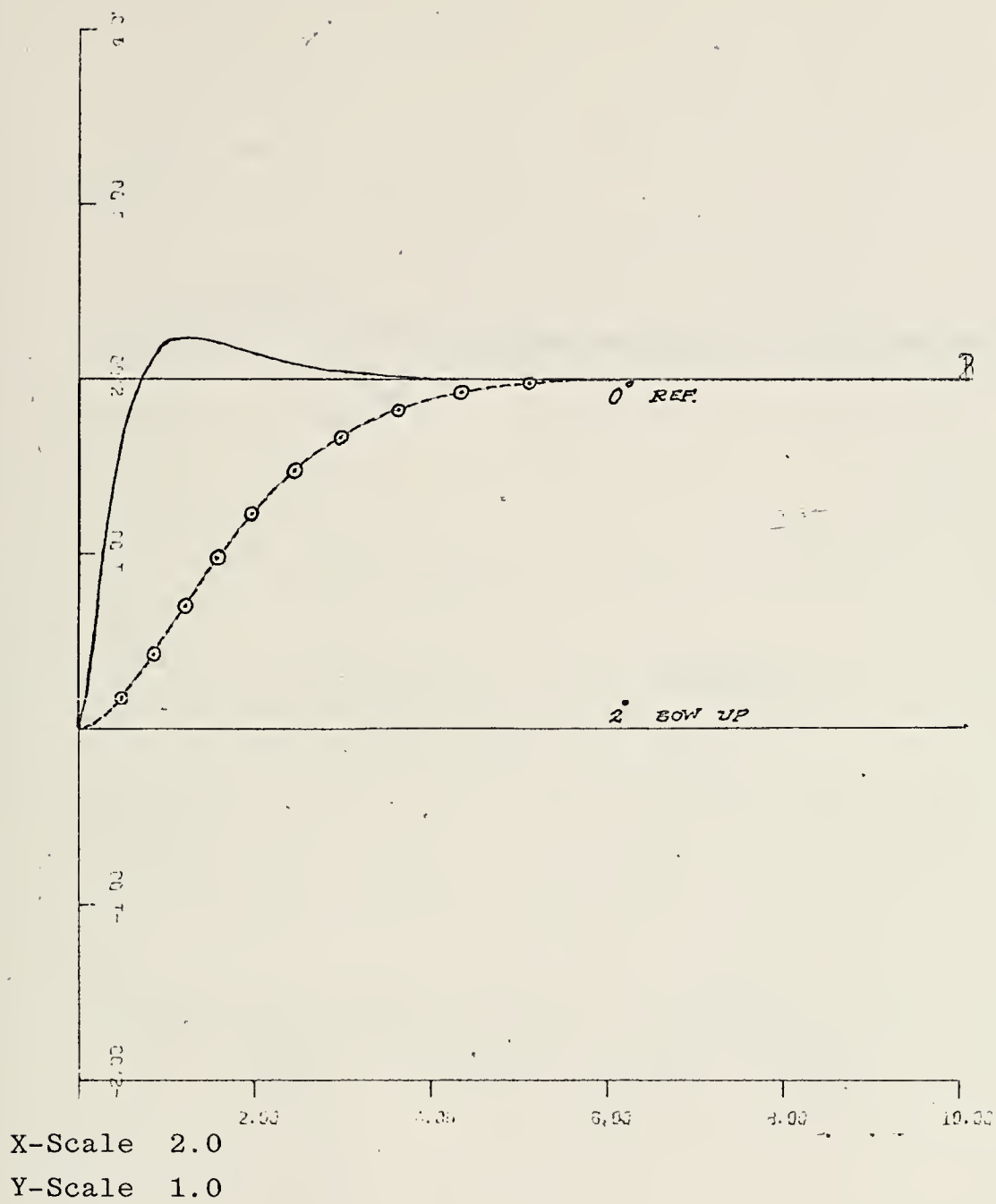
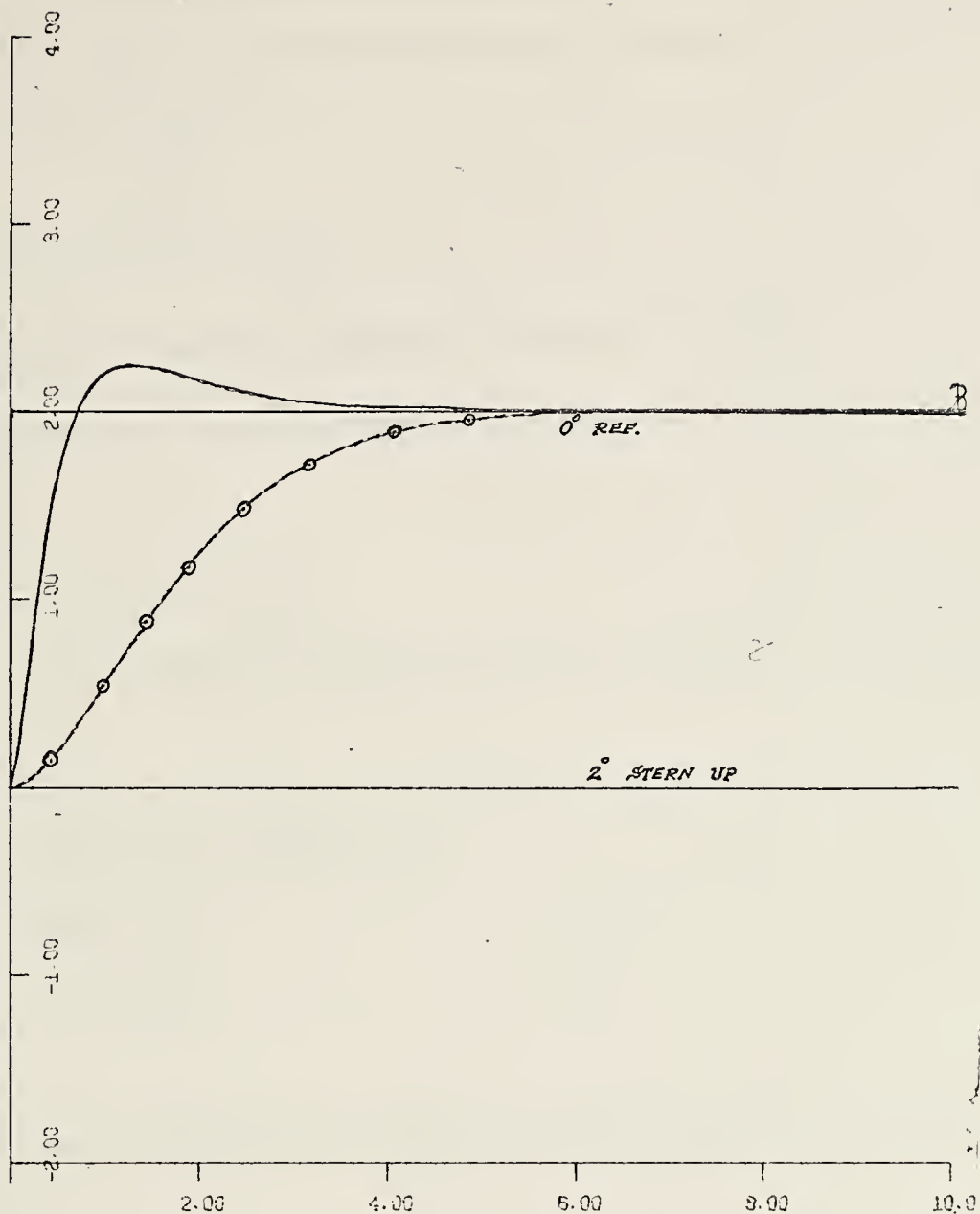


FIGURE 26
STEP RESPONSE OF PITCH ANGLE (BOW UP)



X-Scale 2.0

Y-Scale 1.0

FIGURE 27

STEP RESPONSE OF PITCH ANGLE (STERN UP)

C. ROOT LOCUS DESIGN FOR ROLL MODE

After neglecting the small terms, equation (2-4) becomes

$$\dot{P} = \frac{1}{I_{XX}} \cdot L$$

And from equation (2-41)

$$L = F_{ZPF}L_{YPF} + F_{ZSF}L_{YSF} - F_{YPS}L_{ZPS} - F_{YSS}L_{ZSS} - F_{YCS}L_{ZCS}$$

Assume that the roll mode was decoupled from the other modes

$$L = F_{ZPF}L_{YPF} + F_{ZSF}L_{YSF}$$

$$= [-D_2(0.0028A_2 + 0.018)\delta_P]L_{YPF} + [-D_2(0.0028A_2 + 0.018)\delta_S]L_{YSF}$$

$$\delta_P = -\delta_S$$

$$L = -29959.4\delta_S + (-29959.4\delta_S)$$

$$= -59918.8\delta_S$$

$$\dot{P} = \ddot{\phi} = -0.1\delta_S$$

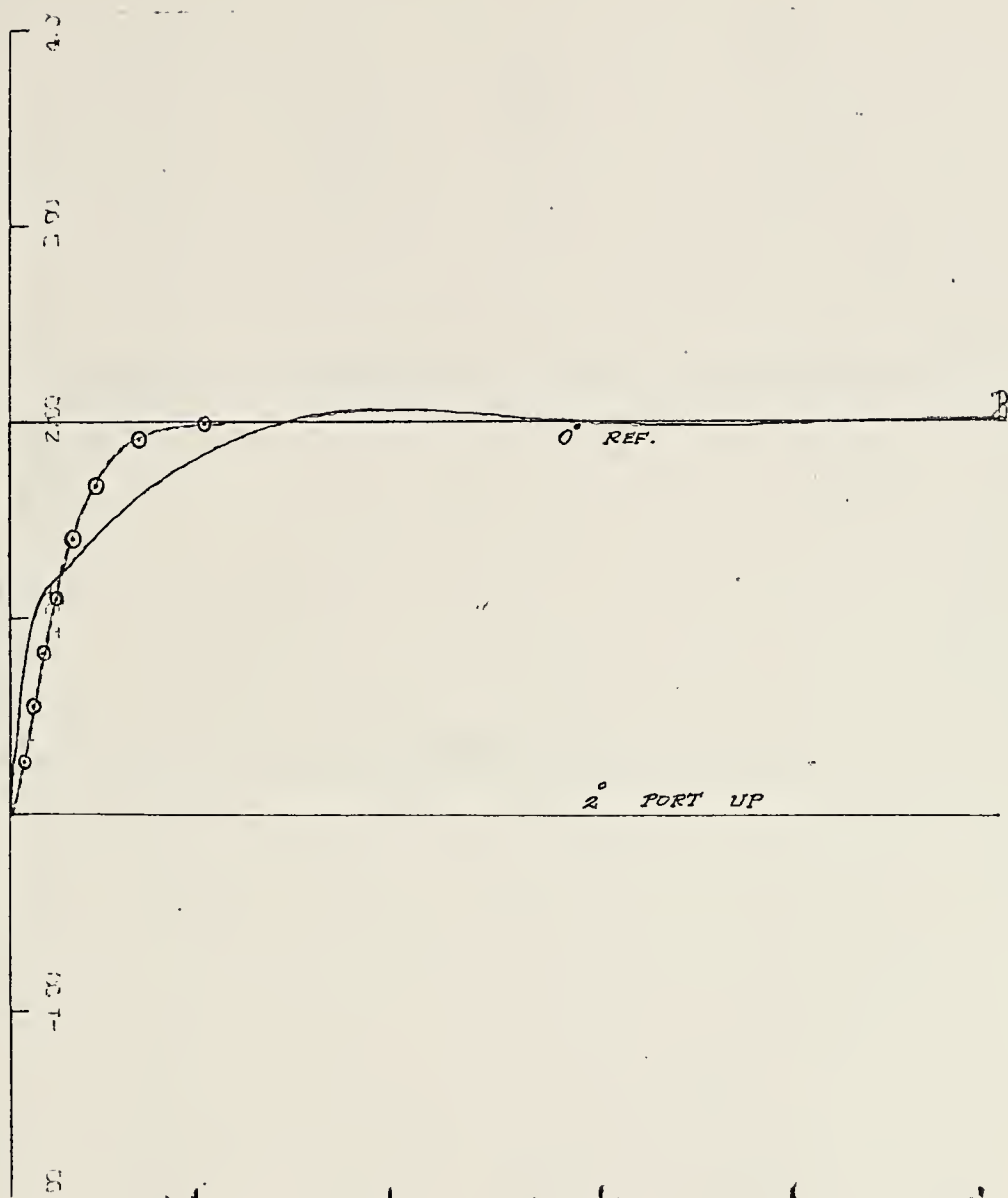
Taking the Laplace Transform, the transfer function is simply

$$\frac{\phi}{\delta_S} = -\frac{0.1}{S^2} \quad (4-20)$$

Figure 28 is the root locus plot after compensation using a lead network which has zero at -1.5 and pole at -15. With the gain of -82, the roots were at $-3.5 \pm j0.75$, which gave the value of $\zeta = 0.96$ and $\omega_n = 3.6$. Figure 29 is the step response roll from 2° port up back to 0° reference and

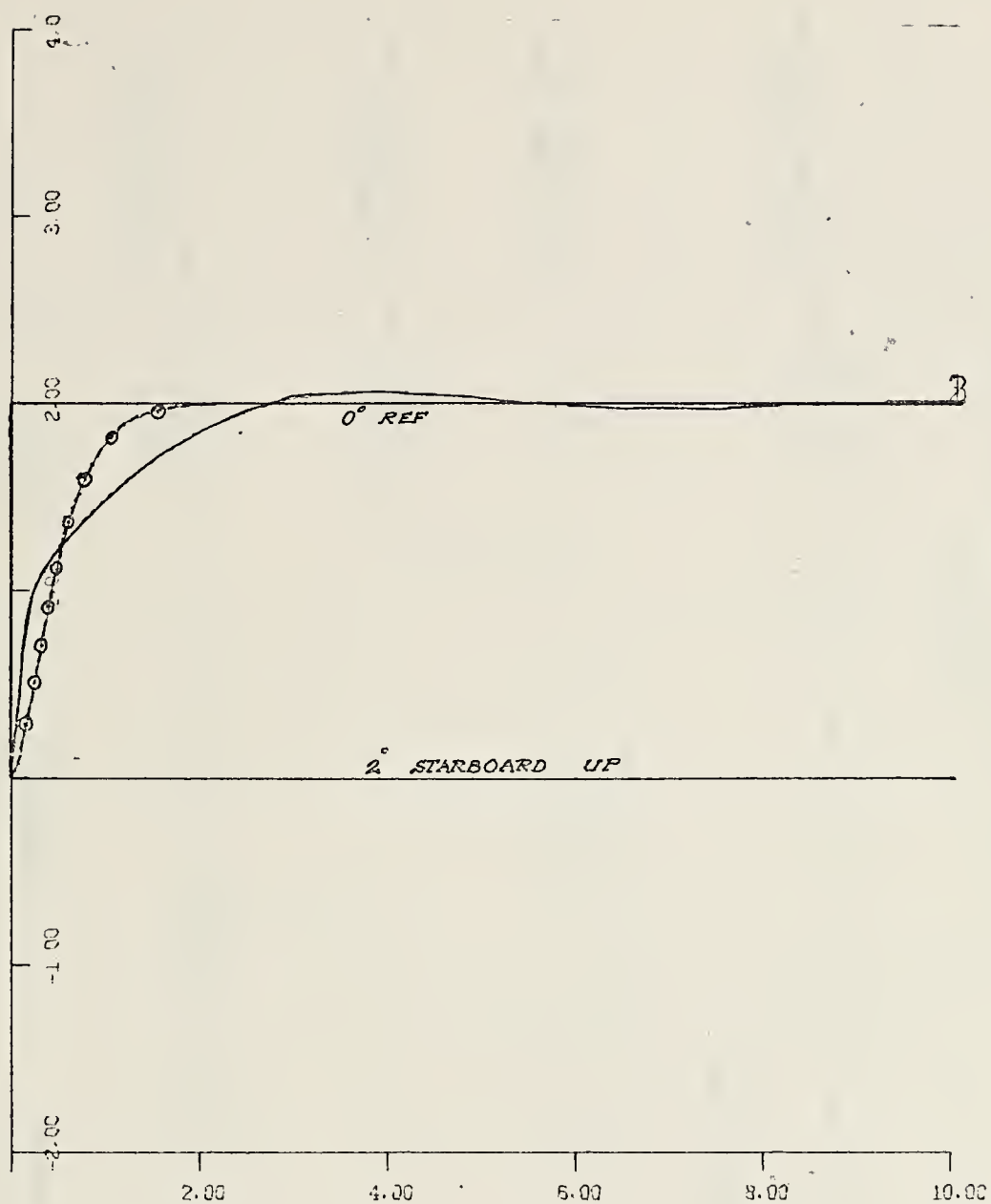
Figure 30 from 2° starboard up to 0° reference. The same response is obtained in both cases. The block diagram of the automatic control of this system is shown in Figure 31.





X-Scale 2.0
Y-Scale 1.0

FIGURE 29
STEP RESPONSE OF ROLL ANGLE (PORT UP)



X-Scale 2.0

Y-Scale 1.0

FIGURE 30
STEP RESPONSE OF ROLL ANGLE (STARBOARD UP)

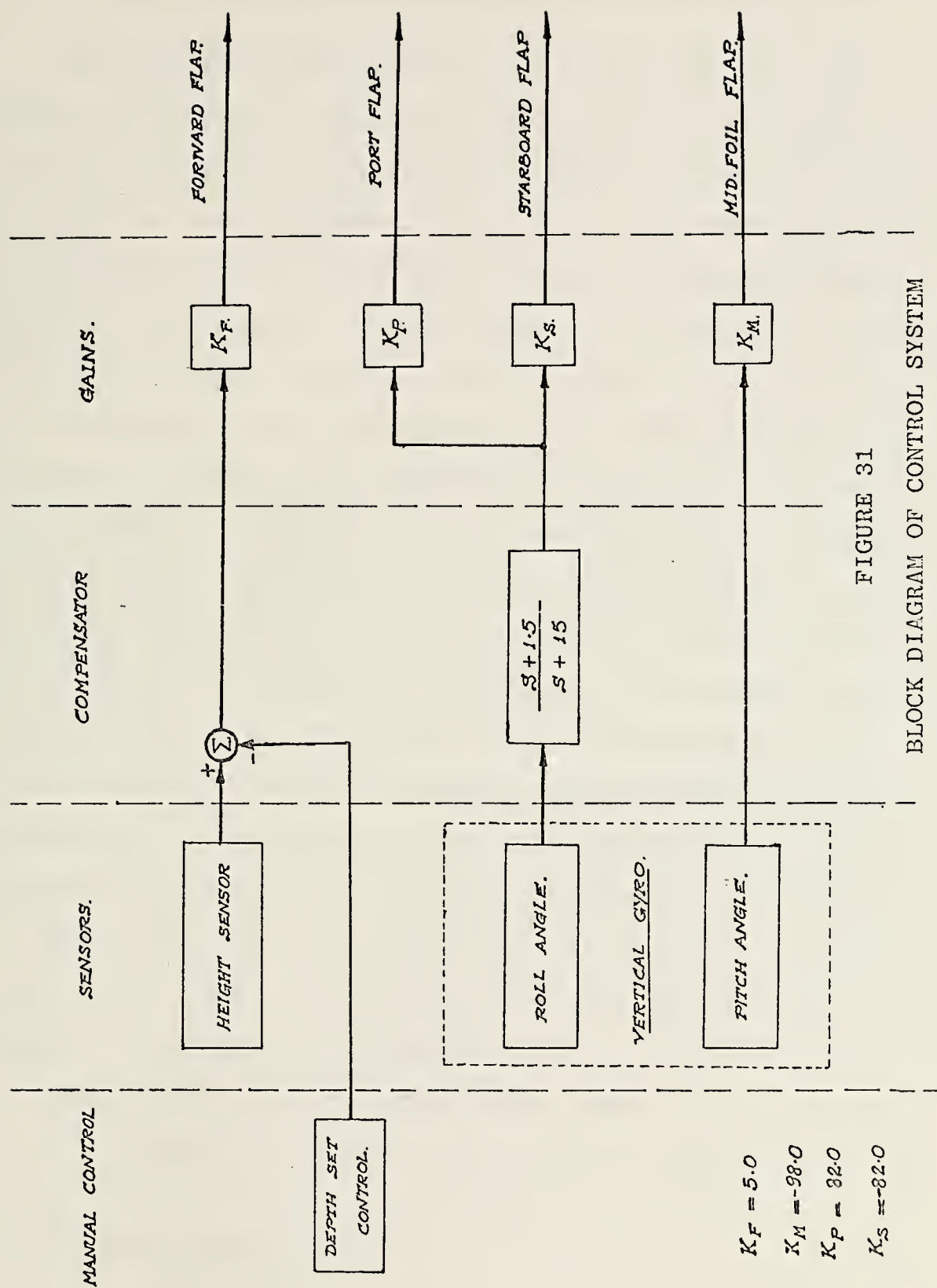


FIGURE 31
BLOCK DIAGRAM OF CONTROL SYSTEM

VI. CONCLUSIONS AND RECOMMENDATIONS FOR FURTHER STUDY

The transfer functions and root locus study has shown that this system is unstable by itself because of the open loop pole in the right half plane. From studying the effect of each foil on the system, it has been shown that stabilization can be achieved by simply closing each loop and using the appropriate gain. However, that will stabilize only the effect of one foil when the other is fixed.

To stabilize the systems when both forward and aft foils are used, the total system has been treated as a multivariable system. To reduce the work in designing the automatic control system, some assumptions had to be made, such as no coupling between the pitch-heave modes, roll mode and yaw mode. Thus, the system will have only a 2×2 transfer function matrix for the pitch-heave mode, and single loop for the roll mode. The step response study has shown that the responses of the compensated system followed closely the response of the best second order approximation. The system was made stable in both pitch-heave and roll mode. However this result cannot insure that the system is completely stable in six degrees of freedom.

Recommendations for further study are:

- 1) Study of yaw motion and the craft turning characteristic
- 2) Wind effects

- 3) Produce a simulation for the transition period between hullborne and foilborne
- 4) Take the dynamic characteristic of the sensors into account
- 5) Study the response of the craft in a sinusoidal sea and in a random sea.

APPENDIX A

SUMMARY OF COMPLETE EQUATIONS

EQUATIONS FOR ACCELERATION IN BODY AXIS

$$\dot{U} = \frac{1}{m}F_X + RV - QW \quad (A-1)$$

$$\dot{V} = \frac{1}{m}F_Y + PW - RU \quad (A-2)$$

$$\dot{W} = \frac{1}{m}F_Z + QU - PV \quad (A-3)$$

$$\dot{P} = \frac{1}{I_{XX}}[L - QR(I_{ZZ} - I_{YY}) + (\dot{R} + QP)I_{XZ}] \quad (A-4)$$

$$\dot{R} = \frac{1}{I_{YY}}[N - PQ(I_{YY} - I_{XX}) - (QR - \dot{P})I_{XZ}] \quad (A-5)$$

VELOCITY IN BODY AXES

$$U = \int \dot{U} dt \quad (A-6)$$

$$V = \int \dot{V} dt \quad (A-7)$$

$$W = \int \dot{W} dt \quad (A-8)$$

$$P = \int \dot{P} dt \quad (A-9)$$

$$Q = \int \dot{Q} dt \quad (A-10)$$

$$R = \int \dot{R} dt \quad (A-11)$$

TRANSFORMATION OF VELOCITIES FROM BODY TO EARTH AXES

$$U_E = U \cos \theta \cos \psi + V(\cos \psi \sin \theta \sin \phi - \sin \psi \cos \phi) + W(\cos \psi \sin \theta \cos \phi + \sin \psi \sin \phi) \quad (A-12)$$

$$V_E = U \cos \theta \sin \psi + V(\cos \psi \cos \phi + \sin \psi \sin \theta \sin \phi) + W(\sin \psi \sin \theta \cos \phi - \cos \psi \sin \phi) \quad (A-13)$$

$$W_E = -U \sin \theta + V \cos \theta \sin \phi + W \cos \theta \cos \phi \quad (A-14)$$

$$\dot{\phi} = P + \dot{\psi} \sin \theta \quad (\text{A-15})$$

$$\dot{\theta} = Q \cos \phi - R \sin \phi \quad (\text{A-16})$$

$$\dot{\psi} = (Q \sin \phi + R \cos \phi) \cos \theta + (\dot{\phi} - P) \sin \theta \quad (\text{A-17})$$

POSITION IN EARTH AXES

$$X_E = \int U_E dt \quad (\text{A-18})$$

$$Y_E = \int V_E dt \quad (\text{A-19})$$

$$Z_E = \int W_E dt \quad (\text{A-20})$$

$$\phi = \int \dot{\phi} dt \quad (\text{A-21})$$

$$\theta = \int \dot{\theta} dt \quad (\text{A-22})$$

$$\psi = \int \dot{\psi} dt \quad (\text{A-23})$$

EXPANSION OF FORCE AND MOMENT EQUATIONS

$$F_X = \Sigma F_{XIF} + \Sigma F_{XIS} + mg_X + T_X \quad (\text{A-24})$$

$$F_Y = \Sigma F_{YIS} + mg_Y \quad (\text{A-25})$$

$$F_Z = \Sigma F_{ZIF} + mg_Z \quad (\text{A-26})$$

$$L = (F_Z L_Y)_{PF} + (F_Z L_Y)_{SF} - (F_Y L_Z)_{PS} - (F_Y L_Z)_{SS} - (F_Y L_Z)_{CS} \quad (\text{A-27})$$

$$M = \Sigma (F_Z L_X)_{IF} + \Sigma (F_X L_Z)_{IF} + \Sigma (F_X L_Z)_{IS} + T_X L_{ZT} \quad (\text{A-28})$$

$$N = \Sigma (F_Y L_X)_{IS} \quad (\text{A-29})$$

EXPANSION OF GRAVITY TERMS

$$mg_X = -mg \sin \theta \quad (\text{A-30})$$

$$mg_Y = mg \cos \theta \sin \phi \quad (\text{A-31})$$

$$mg_Z = mg \cos \theta \sin \phi \quad (\text{A-32})$$

FOIL VELOCITY COMPONENTS IN BODY AXES

Center Foil:

$$U_C = U + L_{ZCF} \cdot Q \quad (A-33)$$

$$V_C = V - L_{ZCF} \cdot P + L_{XCF} \cdot Q \quad (A-34)$$

$$W_C = W - L_{XCP} \cdot Q \quad (A-35)$$

Port Foil:

$$U_P = U + L_{ZPF} \cdot Q - L_{YPF} \cdot R \quad (A-36)$$

$$V_P = V - L_{ZPF} \cdot P + L_{XPF} \cdot R \quad (A-37)$$

$$W_P = W + L_{YPF} \cdot P - L_{XPF} \cdot Q \quad (A-38)$$

Starboard Foil:

$$U_S = U + L_{ZSF} \cdot Q - L_{YSF} \cdot R \quad (A-39)$$

$$V_S = V - L_{ZSF} \cdot P + L_{XSF} \cdot R \quad (A-40)$$

$$W_S = W + L_{YSF} \cdot P - L_{XSF} \cdot Q \quad (A-41)$$

Mid Foil:

$$U_M = U + L_{XMF} \cdot Q \quad (A-42)$$

$$V_M = V - L_{ZMF} \cdot P + L_{XMF} \cdot R \quad (A-43)$$

$$W_M = W - L_{XMF} \cdot Q \quad (A-44)$$

TRANSFORMATION OF WATER PARTICLE ORBITAL VELOCITY FROM EARTH
TO BODY AXES

$$U_{WI} = U_{EWI} \cos \psi \cos \theta + V_{EWI} \sin \psi \cos \theta - W_{EWI} \sin \theta \quad (A-45)$$

$$V_{WI} = U_{EWI} (\cos \psi \sin \theta \sin \phi - \sin \psi \cos \phi) + V_{WEI} (\sin \psi \sin \theta \sin \phi + \cos \psi \cos \phi) \\ + W_{EWI} \cos \theta \sin \phi \quad (A-46)$$

$$W_{WI} = U_{EWI} (\cos \psi \sin \theta \cos \phi + \sin \psi \sin \phi) + V_{WEI} (\sin \psi \sin \theta \cos \phi - \cos \psi \sin \phi) \\ + W_{EWI} \cos \theta \cos \phi \quad (A-47)$$

Each of these equations must be repeated for each foil.

RELATIVE VELOCITY COMPONENTS

$$U_{RI} = U_I - U_{WI} \quad (A-48)$$

$$V_{RI} = V_I - V_{WI} \quad (A-49)$$

$$W_{RI} = W_I - W_{WI} \quad (A-50)$$

One set of equations for each foil.

ANGLES OF ATTACK AND SIDE SLIP

$$\alpha_I = \arctan W_{RI}/U_{RI} + \alpha_{I-FIXED} \quad (A-51)*$$

$$\beta_I = \arcsin \frac{V_{RI}}{\sqrt{U_{RI}^2 + V_{RI}^2 + W_{RI}^2}} \quad (A-52)*$$

* One set of equations for each foil. Angles of attack and side slip are calculated in radians.

TOTAL RELATIVE VELOCITY AT A PARTICULAR FOIL OR STRUT

$$V = \sqrt{U_R^2 + V_R^2 + W_R^2} \quad (A-53)$$

HYDRODYNAMIC FORCES IN WATER AXES

(Each foil equation and strut equation must be repeated for foil and strut, respectively)

Foil Lift:

$$F_L = \frac{1}{2} \rho V^2 A_F C_F \quad (A-54)$$

Foil Drag:

$$F_{DF} = \frac{1}{2} \rho V^2 A_F C_F \quad (A-55)$$

Strut Drag:

$$F_{DS} = \frac{1}{2} \rho V^2 A_S C_{DS} \quad (A-56)$$

Strut Side Force:

$$F_S = \frac{1}{2} \rho V^2 A_S C_S \quad (A-57)$$

TRANSFORMATION OF FOIL FORCES FROM WATER AXES TO BODY AXES

$$F_{XIF} = -F_{IDF} \cos \alpha \cos \beta + F_{LIF} \sin \alpha \quad (A-58)$$

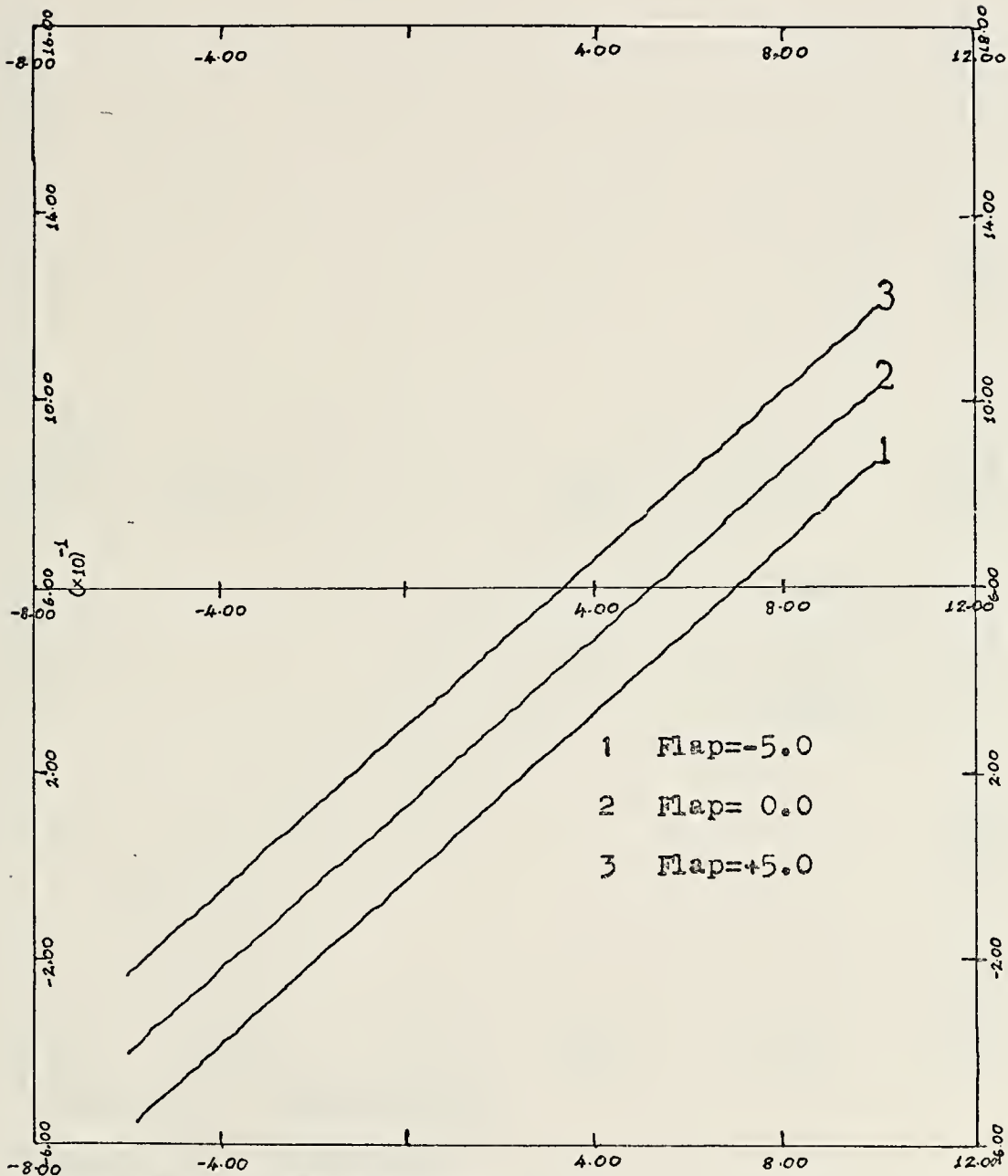
$$F_{YIF} = -F_{DIF} \sin \beta \quad (A-59)$$

$$F_{ZIF} = -F_{DIF} \sin \alpha \cos \beta - F_{LIF} \cos \alpha \quad (A-60)$$

APPENDIX B

PLOTS OF HYDRODYNAMIC COEFFICIENTS

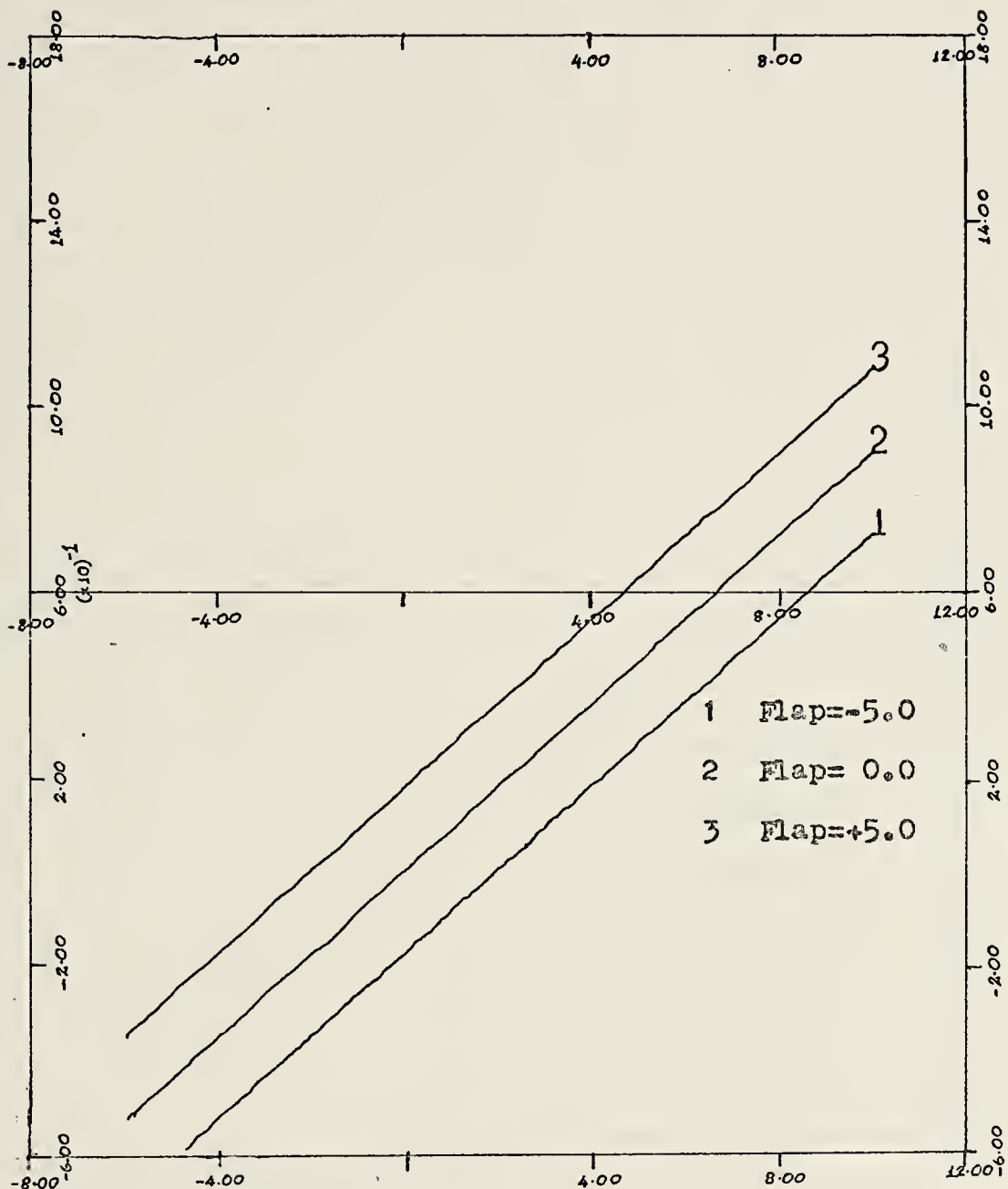
Fwd. Foil Lift Coefficient vs. Angle of Attack



X-Scale 4.0 degrees/Inch

Y-Scale 0.4 Unit/Inch

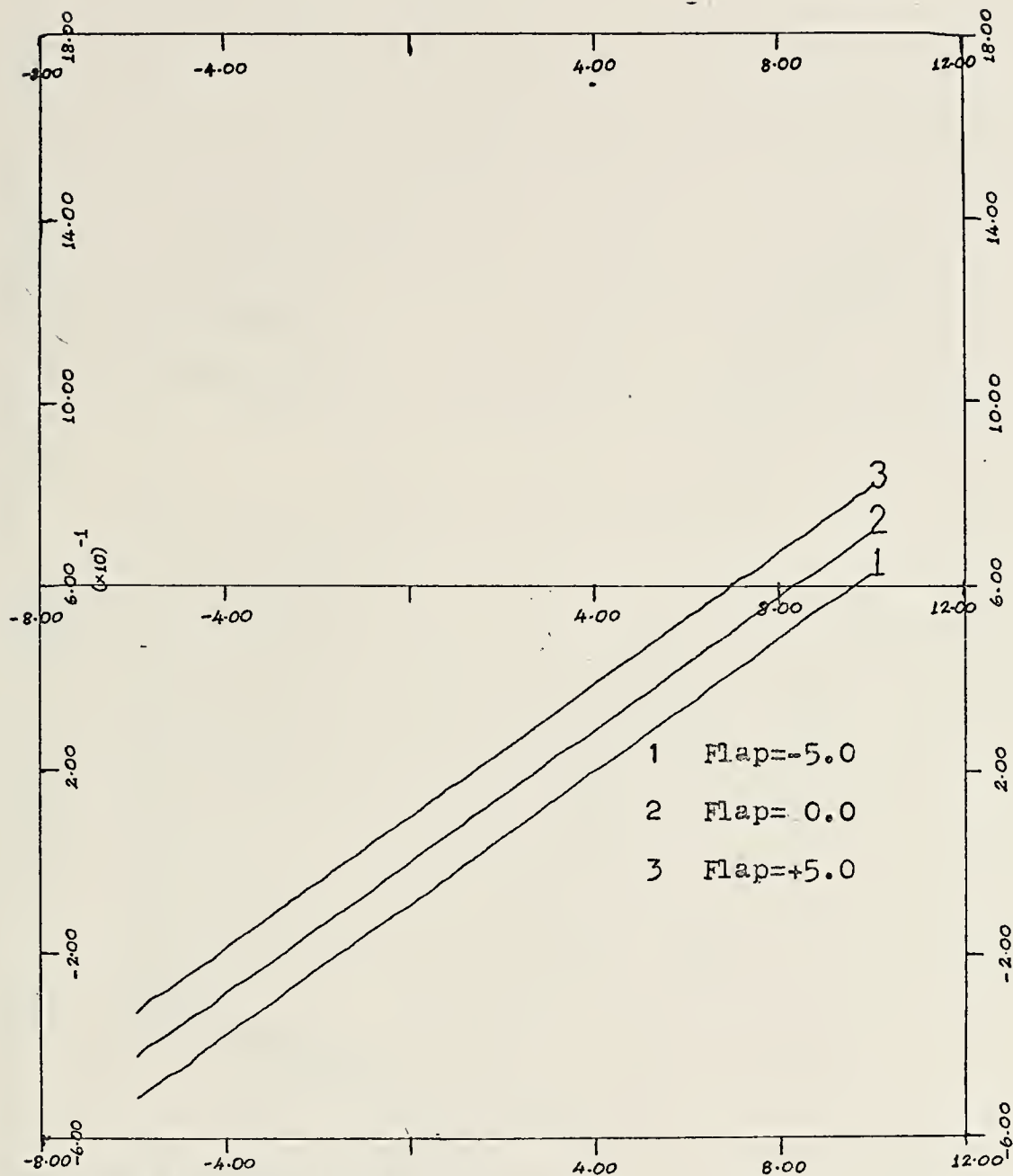
Mid Foil Lift Coefficient vs. Angle of Attack



X-Scale 4.0 Degrees/Inch

Y-Scale 0.4 Unit/Inch

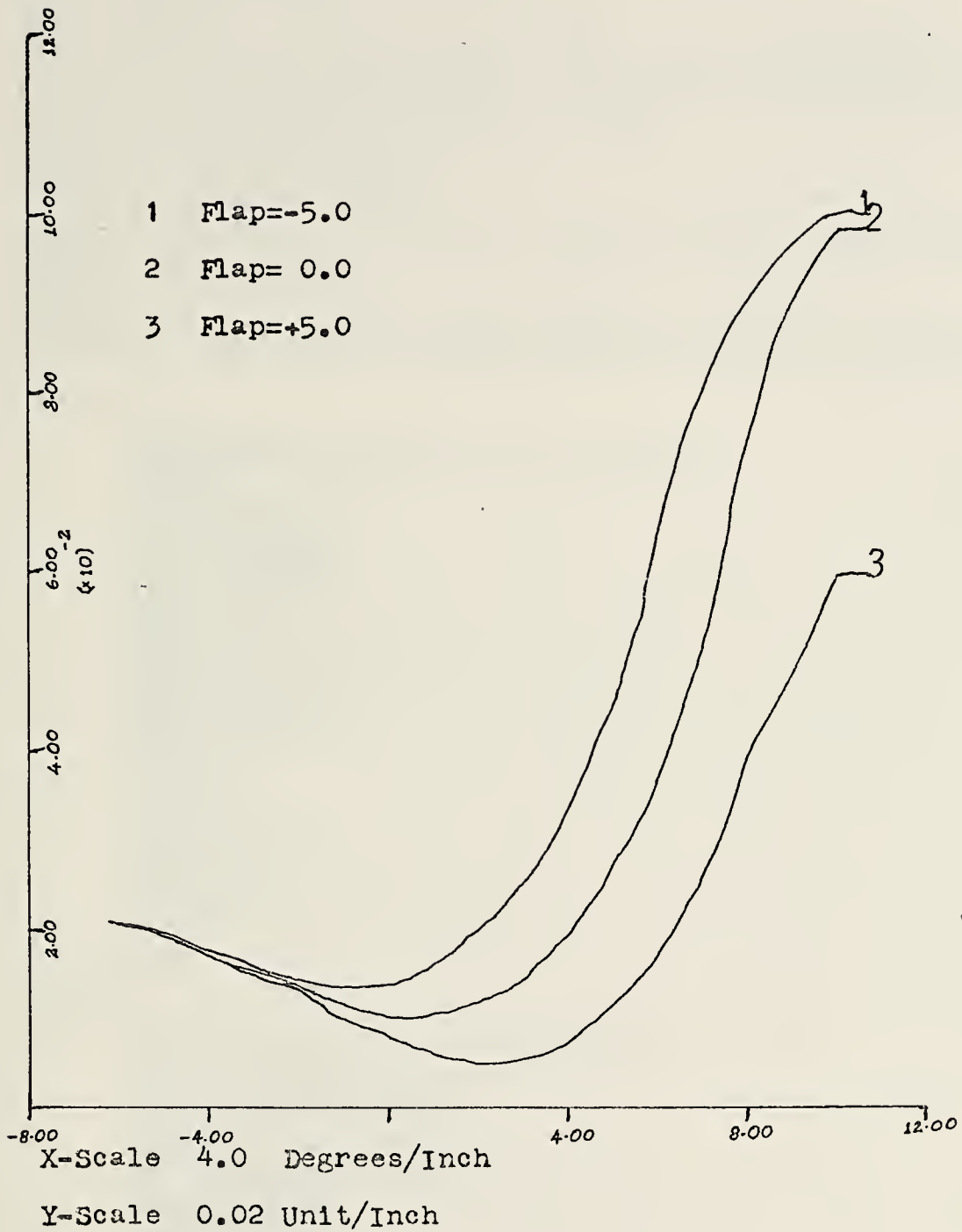
Aft. Foil Lift Coefficient vs. Angle of Attack



X-Scale 4.0 Degrees/Inch

Y-Scale 0.4 Unit/Inch

Forward Foil Drag Coefficient vs. Angle of Attack




```

// EXEC DSL,PARAM.C='NOSOURCE,NOMAP'
//DSL.INPUT DD *
D      COMMON MATRIX(539)
CONTRL FINTIM=10.0,DELT=0.025,DELS=0.05
INTEG  RKSFx
INTEGER IFLAG,IFLAG1,NPLOT,NUM,NCUR
CONST  NPLOT=3,NCUR=1,IFLAG=0
CONST  WEIGHT=262527, IXX=601200, IYY=4286000,...
IZZ=4174000,G=32.2
CONST  ACFP=32.7,ACFS=32.7,APF=36.8,ASF=36.8,AMF=76.0, ...
PI=3.141593
CONST  LXCF=41.59,LXCS=41.59,LXPF=-16.98,LXPS=-16.98,...
LXSF=-16.98,LXSS=-16.98,LXMF=-16.98,LYCP=-5.0,LYCS=5.0,...
LYPF=-12.42,LYPS=-8.0,LYSF=12.42,LYSS=8.0,LZCF=15.5,...
LZCS=13.25,LZPF=17.14,LZPS=14.0,LZSF=17.14,LZSS=14.0,...
LZMF=17.14,LXT=-16.9,LZT=17.7,LXH=68.0
CONST  K1=5.0,K2=-98.0,K3=-82.0
STORAG IC(2),NU(1),DEN(3)
TABLE  IC(1-2)=2*0.0,NU(1)=3.99,DEN(1-3)=1.0,4.0,3.99
PARAM  UZERO=36.0
PREPAR .1,FX,FY,FZ,L,M,N,U,V,W,ZE,P,Q,R,THETA ,UDOT,WDOT,...
QDOT,ALFCP,ALFCS,ZE1,PHI,PHI1,THETA3,X,Y
GRAPH  TIME,THETA3,X,Y
PRPLOT
LABEL  STEP RESPONSE OF PITCH ANGLE
PRINT  0.5,TIME,ZE,PHI,P,PDOT,THETA,ELVP,ELVS,FLAP,ARS,ARP
*
INITIAL
*
      DENSE=2.0
      UINIT=UZERO*2000.0*3.0*1.0/3600.0
      U=UINIT
      TX=3960.0
      ALM=0.074269
      ALS=0.074269
      ALP=0.074269
      ALF=0.037111
      PREF=0.0
      TREF=0.0
      THETA2=-2.0*PI/180.0
      PHI2=0.0
      MASS=WEIGHT/G
      CONV=PI/180.0
      FLAP=0.0
      ELV=0.0
      ARP=0.0
      ARS=0.0
      HREF=11.5
      HREF2=-11.5
      FLAG=0.0
      IFLAG1=0
      EPS=25.0
*
DERIVATIVE
*
NOSORT
*
      ANGLES OF ATTACK AND SIDE SLIP
*
      VRC=V-LZCF*P+LXCF*R
      VRS=V-LZSF*P+LXSF*R
      VRM=V
      VRP=V-LZPF*P+LXPF*R
      WRP=W+LYPF*P-LXPF*Q
      WRS=W+LYSF*P-LXSF*Q
      WRM=W-LXMF*Q
      WRC=W-LXCF*Q
      ALFC=WRC/U+ALF
      ALFAP=WRP/U+ALP
      ALFAS=WRS/U+ALS
      ALFAM=WRM/U+ALM
      BETAC=VRC/U

```



```

BETAP=VRP/U
BETAS=VRS/U

*
*
* CALCULATION OF EULER ANGLES
PHID1=P
THETD1=Q
PSID1=R

*
SORT
THETA=INTGRL(THETA2,THETD1)
PHI=INTGRL(PHI2,PHID1)
PSI=INTGRL(0.0,PSID1)
WE=-U*SIN(THETA)+V*COS(THETA)*SIN(PHI)+W*COS(THETA)...
*COS(PHI)
ZE=INTGRL(HREF2,WE)
ZE1=ZE-HREF2

*
NOSORT
*
*
* SUBMERGENCE TERMS
SECP=ZE-LXCF*THETA+LYCP*SIN(PHI)+LZCF*COS(PHI)
SECS=ZE-LXCF*THETA+LYCS*SIN(PHI)+LZCF*COS(PHI)
SEPF=ZE-LXPF*THETA+LYPF*SIN(PHI)+LZPF*COS(PHI)
SESF=ZE-LXSF*THETA+LYSF*SIN(PHI)+LZSF*COS(PHI)
SEMF=ZE-LXMF*THETA+LZMF*COS(PHI)

*
*
* HYDRODYNAMIC COEFFICIENTS
ELV1=ELV*CONV
ELVD=LIMIT(-5.0,5.0,ELV1)
FLAD=FLAP*CONV
FDEG=LIMIT(-5.0,5.0,FLAD)
ARPD=ARP*CONV
ARPI=LIMIT(-5.0,5.0,ARPD)
ARSD=ARS*CONV
ARS1=LIMIT(-5.0,5.0,ARSD)
CALL INTERP(ALFC,ELVD,COEFC,2)
CALL INTERP(ALFAP,ARPI,COEFPX,3)
CALL INTERP(ALFAS,ARS1,COEFSX,3)
CALL INTERP(ALFAM,FLAP,COEFMX,1)
CALL INTRP1(BETAC,SECF,CFDS,2,THETA,THETA1)
CALL INTRP1(BETAP,SEPF,CPDS,1,THETA,THETA1)
CALL INTRP1(BETAS,SESF,CSDS,1,THETA,THETA1)

*
*
* FORCES IN THE WATER AXES
FGRAX=-MASS*G*SIN(THETA)
FGRAY=MASS*G*SIN(PHI)
FGRAZ=MASS*G*COS(PHI)
CCS=-2.15*BETAC
ACCS=CCS*4.25*SECF
FSC=0.5*DENSE*(U**2)*ACCS
FDSC=0.5*DENSE*(U**2)*CFDS
PCS=-2.15*BETAP
APCS=PCS*4.25*SEPF
FPS=0.5*DENSE*(U**2)*APCS
FDPS=0.5*DENSE*(U**2)*CPDS
SCS=-2.15*BETAS
ASCS=SCS*4.25*SESF
FSS=0.5*DENSE*(U**2)*ASCS
FDSS=0.5*DENSE*(U**2)*CSDS
CLCF=5.15*ALFC+0.036*ELV+0.13
FLC=0.5*DENSE*(U**2)*ACF*CLCF
FDC=0.5*DENSE*(U**2)*ACF*COEFC
CLPF=4.10*ALFAP+0.018*ARP
FLP=0.5*DENSE*(U**2)*APF*CLPF
FDP=0.5*DENSE*(U**2)*APF*COEFPX
CLSF=4.10*ALFAS+0.018*ARS
FLS=0.5*DENSE*(U**2)*ASF*CLSF
FDS=0.5*DENSE*(U**2)*ASF*COEFSX

```



```

CLMF=5.15*ALFAM+0.036*FLAP
FLM=0.5*DENSE*(U**2)*AMF*CLMF
FDM=0.5*DENSE*(U**2)*AMF*COEFMX
FLCZ=0.5*DENSE*(U**2)*ACF*CLCF
FDCZ=0.5*DENSE*(U**2)*ACF*COEFC
FLPZ=0.5*DENSE*(U**2)*APF*CLPF
FDPZ=0.5*DENSE*(U**2)*APF*COEFPX
FLSZ=0.5*DENSE*(U**2)*ASF*CLSF
FDSZ=0.5*DENSE*(U**2)*ASF*COEFSX
FLMZ=0.5*DENSE*(U**2)*AMF*CLMF
FDMZ=0.5*DENSE*(U**2)*AMF*COEFMX

```

TRANSFORMATION TO BODY AXES

```

FXCF=-FDC+ALFC*FLC
FXPF=-FDP+ALFAP*FLP
FXSF=-FDS+ALFAS*FLS
FXMF=-FDM+ALFAM*FLM
FXCS=-FDSC-BETAC*FSC
FXPS=-FDPS-BETAP*FPS
FXSS=-FDSS-BETAS*FSS
FYCS=-BETAC*FDSC+FSC
FYPS=-BETAP*FDPS+FPS
FYSS=-BETAS*FDSS+FSS
FZCF=-FDC*ALFC-FLCZ
FZPF=-FDP*ALFAP-FLPZ
FZSF=-FDS*ALFAS-FLSZ
FZMF=-FDM*ALFAM-FLMZ
LZCS=LZCF-0.4*SECF
LZPS=LZPF-0.4*SEPF
LZSS=LZSF-0.4*SESF

```

```

FXONE=FXCF+FXPF+FXSF+FXMF+FXCS+FXPS+FXSS

```

SUMMATION OF FORCES AND MOMENTS

```

FX=FXONE+FGRAX+TX
UDOT=(1./MASS)*FX-Q*W
IF(IFLAG1.EQ.0) UDOT=0.0
FY=FYCS+FYPS+FYSS+FGRAY
FZ=FZCF+FZPF+FZSF+FZMF+FGRAZ
L=FZPF*LYPF+FZSF*LYSF-FYPS*LZPS-FYSS*LZSS-FYCS*LZCS
MFWD=FZCF*LXCF
M=-MFWD-FZPF*LXPF-FZSF*LXSF-FZMF*LXMF+...
FXCF*LZCF+FXPF*LZPF+FXSF*LZSF+FXMF*LZMF+FXCS...
*LZCS+FXPS*LZPS+FXSS*LZSS+TX*LZT
N=FYCS*LXCS+FYPS*LXPS+FYSS*LXSS

```

VELOCITY INTEGRALS

```

VDOT=(1./MASS)*FY-R*U
WDOT=(1./MASS)*FZ+Q*U
PDOT=(1.0/IXX)*L
QDOT=(1.0/IYY)*M
RDOT=(1.0/IZZ)*N
U=INTGRL(UINIT,UDOT)
V=INTGRL(0.0,VDOT)
W=INTGRL(0.0,WDOT)
P=INTGRL(0.0,PDOT)
Q=INTGRL(0.0,QDOT)
R=INTGRL(0.0,RDOT)

```

AUTOMATIC CONTROL BLOCK

```

HACT=-ZE+LXH*THETA
DELH=HREF-HACT
DETH=TREF-THETA
DEPH=PREF-PHI
ELV=K1*DELH
FLAP=K2*DETH

```



```

      GO TO 2
10  I1=I
    IF(I1.LE.8) I1=I1+1
    J=0
    K=1
    ICOUNT=0
    MATRIX=3
6   IF(I1.GT.8) GO TO 2
    DO 11 I=I1,8
      J=J+1
      IF(J.GT.3) K=K+1
      IF(J.GT.3) J=1
      COEFMX(J,K)=INFO(I)
      ICOUNT=ICOUNT+1
      IC=IC+1
      IF(ICOUNT.EQ.99) GO TO 12
11  CONTINUE
    GO TO 2
12  I1=I
    IF(I1.LE.8) I1=I1+1
    J=0
    K=1
    ICOUNT=0
    MATRIX=4
7   IF(I1.GT.8) GO TO 2
    DO 13 I=I1,8
      J=J+1
      IF(J.GT.11) K=K+1
      IF(J.GT.11) J=1
      CADS1(J,K)=INFO(I)
      ICOUNT=ICOUNT+1
      IC=IC+1
      IF(ICOUNT.EQ.121) GO TO 15
13  CONTINUE
    GO TO 2
15  I1=I
    IF(I1.LE.8) I1=I1+1
    J=0
    K=1
    ICOUNT=0
    MATRIX=5
8   IF(I1.GT.8) GO TO 2
    DO 14 I=I1,8
      J=J+1
      IF(J.GT.11) K=K+1
      IF(J.GT.11) J=1
      CFDS1(J,K)=INFO(I)
      ICOUNT=ICOUNT+1
      IC=IC+1
      IF(ICOUNT.EQ.121) GO TO 16
14  CONTINUE
    GO TO 2
16  IFLAG1=1
    GO TO 2
50  IFLAG=1
    IF((IFLAG.EQ.1).AND.(IFLAG1.EQ.1)) GO TO 52
51  WRITE(6,104) ICOUNT,MATRIX,IC
104 FORMAT(' ','JOB FAILURE',1X,'COUNT=',I6,1X,'MATRIX=',
1I6,1X,'NO.PTS=',I6)
    FLAG=1
    RETURN
52  WRITE(6,105) IC
105 FORMAT(' ','JOB COMPLETE',1X,'POINTS STORED=',I6)
    RETURN
    END

```

FORTRAN

C
C
C
C

SUBROUTINE INTERP

SUBROUTINE INTERP(ALFAC,FLAP,COEF,M)
COMMON COEFMX,COEFCX,COEFOX


```

        DIMENSION COEFMX(3,33),COEFCX(3,33),COEFOX(3,33)
        DATA CONDEG/57.295773/
        ALFA=ALFAC*CONDEG
        IF(ALFA.GT.10.0) WRITE(6,100)ALFAC,M
        IF(ALFA.GT.10.0) ALFA=10.0
100  FORMAT('0','ERROR.ALFA EXCEEDED LIMITS.ALFA=',E14.8,
        12X,'M=',I1)
        IF(ALFA.LT.-6.0) WRITE(6,100) ALFAC,M
        IF(ALFA.LT.-6.0) ALFA=-6.0
        ALPHA=2.0*ALFA
        IF(ALPHA.LT.0.0) GO TO 1
        IF(ALPHA.GT.0.0) GO TO 2
        IA=13
        WTA=0.0
        GO TO 3
1  IA1=-ALPHA
   IA=13-IA1
   ALPHA1=-IA1
   WTA=ALPHA-ALPHA1
   GO TO 3
2  IA1=ALPHA
   IA=13+IA1
   ALPHA1=IA1
   WTA=ALPHA-ALPHA1
3  IF(FLAP.LT.-5.0) WRITE(6,101) FLAP
   IF(FLAP.LT.-5.0) FLAP=-5.0
   IF(FLAP.GT.5.0) WRITE(6,101) FLAP
   IF(FLAP.GT.5.0) FLAP=5.0
101 FORMAT('0','ERROR.FLAP EXCEEDED LIMITS.FLAP=',E14.8)
   IF(FLAP)4,5,6
4  IB=1
   WTB=-((5.0+FLAP)/5.0)
   GO TO 7
5  IB=2
   WTB=0.0
   GO TO 7
6  IB=3
   WTB=(5.0-FLAP)/5.0
7  IF(WTA)8,9,10
8  IA2=IA-1
   GO TO 11
9  IA2=IA
   GO TO 11
10 IA2=IA+1
11 IF(WTB)12,13,12
12 IB2=2
   GO TO 14
13 IB2=IB
14 GO TO(15,16,17),M
15 COEF1=COEFMX(IB,IA)
   COEF2=COEFMX(IB2,IA)
   GO TO 18
16 COEF1=COEFCX(IB,IA)
   COEF2=COEFCX(IB2,IA)
   GO TO 18
17 COEF1=COEFOX(IB,IA)
   COEF2=COEFOX(IB2,IA)
18 COEF3=(COEF2-COEF1)*ABS(WTB)+COEF1
   GO TO (19,20,21),M
19 COEF1P=COEFMX(IB,IA2)
   COEF2P=COEFMX(IB2,IA2)
   GO TO 22
20 COEF1P=COEFCX(IB,IA2)
   COEF2P=COEFCX(IB2,IA2)
   GO TO 22
21 COEF1P=COEFOX(IB,IA2)
   COEF2P=COEFOX(IB2,IA2)
22 COEF3P=(COEF2P-COEF1P)*ABS(WTB)+COEF1P
   COEF=(COEF3P-COEF3)*ABS(WTA)+COEF3
   RETURN
   END
FORTRAN

```


C
C
C
C

SUBROUTINE INTRP1

```

SUBROUTINE INTRP1(BETA1,SOB,COEFS,M,THETA,THETA1)
COMMON JUNK,CFDS1,CADS1
DIMENSION JUNK(297),CFDS1(11,11),CADS1(11,11)
DATA CONDEG/57.295773/
SUB=SOB
BETA=BETA1*CONDEG
IF(BETA.GT.5.0) WRITE(6,100) BETA1,M
IF(BETA.GT.5.0) BETA=5.0
100 FORMAT('0','ERROR.BETA EXCEEDS LIMITS.BETA=',E14.8,2X,
1 'M=',I1)
IF(BETA.LT.-5.0) WRITE(6,100) BETA1,M
IF(BETA.LT.-5.0) BETA=-5.0
IF(BETA.LT.0.0) GO TO 1
IF(BETA.GT.0.0) GO TO 2
IA=6
WTA=0.0
GO TO 3
1 IA1=-BETA
IA=6-IA1
BETAG=-IA1
WTA=BETA-BETAG
GO TO 3
2 IA1=BETA
IA=6+IA1
BETAG=IA1
WTA=BETA-BETAG
3 IF(SUB.LT.0.0) SUB=0.0
IF(SUB.GT.10.0) SUB=10.0
IF(SUB.GT.0.0) GO TO 5
IS=1
WTS=0.0
GO TO 7
5 IS1=SUB
IS=IS1+1
SUB1=IS1
WTS=SUB-SUB1
7 IF(WTA)8,9,10
8 IA2=IA-1
GO TO 11
9 IA2=IA
GO TO 11
10 IA2=IA+1
11 IF(WTS.GT.0.0) GO TO 12
IS2=IS
GO TO 15
12 IS2=IS+1
15 IF(M.EQ.2) GO TO 16
COEF1=CADS1(IS,IA)
COEF2=CADS1(IS2,IA)
GO TO 18
16 COEF1=CFDS1(IS,IA)
COEF2=CFDS1(IS2,IA)
18 COEF3=(COEF2-COEF1)*WTS+COEF1
IF(M.EQ.2) GO TO 20
19 COEF1P=CADS1(IS,IA2)
COEF2P=CADS1(IS2,IA2)
GO TO 22
20 COEF1P=CFDS1(IS,IA2)
COEF2P=CFDS1(IS2,IA2)
22 COEF3P=(COEF2P-COEF1P)*WTS+COEF1P
COEFS=(COEF3P-COEF3)*ABS(WTA)+COEF3
THETA1=THETA*CONDEG
RETURN
END
//L.SYSLIB DD DISP=SHR,DSN=SYS1.DSL,
// VOL=SER=MARY,UNIT=2314
// DD DISP=SHR,DSN=SYS1.FORTLIB
// DD DISP=SHR,DSN=SYS1.MPSLIB

```



```

//G.FT06F001 DD SPACE=(CYL,(3))
//G.FT03F001 DD DSN=S1269.GLOP,UNIT=2321,DISP=SHR,
//          VOL=SER=CELO04,LABEL=(,,,IN)
//PLOT.SYSIN DD *
STEP RESPONSE OF PITCH ANGLE
NANAGARA
0.0          2.0          -2.0          1.          5.0          6.0

```


LIST OF REFERENCES

1. A thesis, Simulation of Hydrofoil Performance in Calm Water, by Gary Dee Hickox.
2. The Boeing Company Report U 141949, Foilborne Equations of Motion, by J.J. Jamieson, December 1966.
3. The Boeing Company Report U 141948, Performance Criteria and Test Report for Hydrofoil Craft, by J.J. Jamieson, December 1966.
4. The Boeing Company Report U 141951, Equations and Methods for Simulation of Hull Lift, Drag, and Pitch Moment, by J.J. Jamieson, December 1966.
5. The Boeing Company Report U 141952, Hydrofoil Simulation Equations Study, by J.J. Jamieson, December 1966.
6. The Boeing Company Report U 150981. PHM, Foilborne Ship Motion Simulation Equations, by R.H. Mitchell and J.A. Hirsch, 16 August 1972.
7. Naval Ship Research and Development Center, Users Guide Digital Simulation of Hydrofoil Craft (PC(H)-1), by J.E. Russ and V.J. Ryba, January 1971.
8. Abkowitz, M.A., Stability and Motion Control of Ocean Vehicles, M.I.T. Press, 1969.
9. The Research Report Prepared for Ames Research Center, NASA, Moffett Field, California, Steady-State Decoupling and Design of Linear Multivariable Systems, by Jen-Yen Huang, June 1974.
10. A thesis, Height Control of Hydrofoil Craft Employing Completely Submerged Foils, by Donald R. Stark, 1964.

INITIAL DISTRIBUTION LIST

	No. Copies
1. Defense Documentation Center Cameron Station Alexandria, Virginia 22314	2
2. Library, Code 0212 Naval Postgraduate School Monterey, California 93940	2
3. Department Chairman, Code 52 Department of Electrical Engineering Naval Postgraduate School Monterey, California 93940	2
4. Professor George J. Thaler, Code 52Tr Department of Electrical Engineering Naval Postgraduate School Monterey, California 93940	5
5. Professor Alex Gerba, Jr., Code 52Gz Department of Electrical Engineering Naval Postgraduate School Monterey, California 93940	1
6. Professor Milton L. Wilcox, Code 52Wx Department of Electrical Engineering Naval Postgraduate School Monterey, California 93940	1
7. Dr. John H. Slaughter Naval Electronics Laboratory Center San Diego, California 92152	1
8. Mr. Walter Blumberg Naval Ship Research Development Center Annapolis, Maryland 21402	1
9. Mr. Joseph Russ Naval Ship Research Development Center Carderock Laboratory Bethesda, Maryland 20034	1
10. Library, Planning & Design Division Thai Naval Shipyard Bangkok, THAILAND	1



- | | | |
|-----|--|---|
| 11. | Education Section
Personal Department
Royal Thai Navy
Bangkok, THAILAND | 1 |
| 12. | Library, Naval Officer School
Royal Thai Navy
Bangkok, THAILAND | 1 |
| 13. | Library, Royal Thai Naval Academy
Smudhprakarn, THAILAND | 1 |
| 14. | Rear Admiral Prapat Chantakate
Military Research and Development Center
Klongtuay
Bangkok, THAILAND | 1 |
| 15. | Lieutenant Jitt Na Nagara, RTN
48 Sukumvit 81 (Siripoj)
Prakanong, BKK11
Bangkok, THAILAND | 2 |

Thesis

157427

N13 Na Nagara

c.1 The simulation of
hydrofoil performance.

20 JAN 77
15 MAY 83

24030
28355

Thesis

157427

N13 Na Nagara

c.1 The simulation of
hydrofoil performance.

thesN13

The simulation of hydrofoil performance.



3 2768 000 99251 5

DUDLEY KNOX LIBRARY